The Journal of Immunology

RESEARCH ARTICLE | SEPTEMBER 15 2010

# Existence of CD8α-Like Dendritic Cells with a Conserved Functional Specialization and a Common Molecular Signature in Distant Mammalian Species

Vanessa Contreras; ... et. al

*J Immunol* (2010) 185 (6): 3313–3325.
https://doi.org/10.4049/jimmunol.1000824

# Existence of CD8α-Like Dendritic Cells with a Conserved Functional Specialization and a Common Molecular Signature in Distant Mammalian Species

**Vanessa Contreras,* Céline Urien,* Rachel Guiton,[†,‡,§] Yannick Alexandre,* Thien-Phong Vu Manh,[†,‡,§] Thibault Andrieu,[¶] Karine Crozat,[†,‡,§] Luc Jouneau,* Nicolas Bertho,* Mathieu Epardaud,[*,1] Jayne Hope,[‖] Ariel Savina,[#] Sebastian Amigorena,[#] Michel Bonneau,** Marc Dalod,[†,‡,§,2] and Isabelle Schwartz-Cornil[*,2]**

**The mouse lymphoid organ-resident CD8α$^+$ dendritic cell (DC) subset is specialized in Ag presentation to CD8$^+$ T cells. Recent evidence shows that mouse nonlymphoid tissue CD103$^+$ DCs and human blood DC Ag 3$^+$ DCs share similarities with CD8α$^+$ DCs. We address here whether the organization of DC subsets is conserved across mammals in terms of gene expression signatures, phenotypic characteristics, and functional specialization, independently of the tissue of origin. We study the DC subsets that migrate from the skin in the ovine species that, like all domestic animals, belongs to the Laurasiatheria, a distinct phylogenetic clade from the supraprimates (human/mouse). We demonstrate that the minor sheep CD26$^+$ skin lymph DC subset shares significant transcriptomic similarities with mouse CD8α$^+$ and human blood DC Ag 3$^+$ DCs. This allowed the identification of a common set of phenotypic characteristics for CD8α-like DCs in the three mammalian species (i.e., SIRP$^{lo}$, CADM1$^{hi}$, CLEC9A$^{hi}$, CD205$^{hi}$, XCR1$^{hi}$). Compared to CD26$^-$ DCs, the sheep CD26$^+$ DCs show 1) potent stimulation of allogeneic naive CD8$^+$ T cells with high selective induction of the *Ifnγ* and *Il22* genes; 2) dominant efficacy in activating specific CD8$^+$ T cells against exogenous soluble Ag; and 3) selective expression of functional pathways associated with high capacity for Ag cross-presentation. Our results unravel a unifying definition of the CD8α$^+$-like DCs across mammalian species and identify molecular candidates that could be used for the design of vaccines applying to mammals in general.** ***The Journal of Immunology*****, 2010, 185: 3313–3325.**

Migratory and lymphoid organ-resident dendritic cells (DCs) include several DC subtypes that are endowed with specific functions involved in the establishment of tolerance or immunity. The plasmacytoid DC (pDC) subset is a professional producer of the antiviral cytokines IFN-α and IFN-β (1). In the mouse, the CD11c$^{hi}$ lymphoid tissue conventional DCs (LT-DCs) can be divided into CD8α$^+$ and CD11b$^+$ subsets (reviewed in Refs. 2, 3). CD11b$^+$ LT-DCs are generally more efficient than the CD8α$^+$ DCs at MHC class II Ag presentation (4–6). Conversely, in most instances, the CD8α$^+$ DCs are more capable than the CD11b$^+$ DCs for cross-priming CD8$^+$ T cells after the processing of endocytosed exogenous or self Ags (6, 7). This functional specialization of the CD8α$^+$ DCs for CD8$^+$ T cell activation relies on a number of intrinsic molecular properties. First, CD8α$^+$ LT-DCs express several components of the molecular machinery for MHC class I Ag processing and presentation to higher levels than CD11b$^+$ LT-DCs (6). They produce high levels of biologically active IL-12, which contributes to promote the activation and the functional polarization of CD8$^+$ T cells toward polyfunctional effector or memory subsets (6, 8). They show a higher efficiency for uptake of apoptotic bodies (9) due to their selective expression of certain scavenger receptors. They express high levels of the CLEC9A protein, which routes engulfed dead cell fragments toward a specialized phago-/endosomal compartment dedicated to cross-presentation (10, 11). They also display a tight control of the phago-/endosomal acidification that is related to moderate activity in Ag degradation (12). Finally, they have the ability to export engulfed materials to the cytosol (13). Recently, a similar

*Virologie et Immunologie Moléculaires UR892; **Centre de Recherche en Imagerie Interventionnelle, Institut National de la Recherche Agronomique, Domaine de Vilvert, Jouy-en-Josas; [†]Centre d'Immunologie de Marseille-Luminy, Université de la Méditerranée, Parc Scientifique et Technologique de Luminy; [‡]Institut National de la Santé et de la Recherche Médicale U631; [§]Centre National de la Recherche Scientifique, Unité Mixte de Recherche 6102, Marseille; [¶]Centre d'Energie Atomique, Division of Immuno-Virology, Direction des Sciences du Vivant, Institut des Maladies Emergentes et des Thérapies Innovantes, Fontenay-aux-Roses; [#]Institut Curie, Paris, France; and [‖]Institute for Animal Health, Compton, United Kingdom

[1]Current address: Institut National de la Recherche Agronomique-Centre International de la Recherche Agronomique pour le Développement, Unité Mixte de Recherche 1309, Campus International de Baillarguet, Montpellier, France.

[2]M.D. and I.S.-C. are cosenior authors.

Received for publication March 12, 2010. Accepted for publication July 2, 2010.

This work was supported by Agence Nationale pour la Recherche Grants ANR 06 GANI 015-03 and ANR Blanc 13000288, ARC (research grant to M.D.), Centre National de la Recherche Scientifique (postdoctoral fellowship to R.G.), and institutional grants to the Centre d'Immunologie de Marseille-Luminy.

The microarray gene expression data presented in this article have been submitted to Gene Expression Omnibus under accession number GSE21889.

Address correspondence and reprint requests to Dr. Isabelle Schwartz-Cornil and Dr. Marc Dalod, Virologie et Immunologie Moléculaires UR892, Institut National de la Recherche Agronomique, Domaine de Vilvert, 78352 Jouy-en-Josas Cedex, France (I.S.-C.) and Centre d'Immunologie de Marseille-Luminy, Université de la Méditerranée, Parc Scientifique et Technologique de Luminy, 13288 Marseille, France (M.D.). E-mail addresses: isabelle.schwartz@jouy.inra.fr (I.S.-C.) and dalod@ciml.univ-mrs.fr (M.D.)

The online version of this article contains supplemental material.

Abbreviations used in this paper: BATF3, basic leucine zipper transcription factor ATF-like 3; BDCA, blood DC Ag; BHK, baby hamster kidney; BTV, bluetongue virus; CADM1, cell adhesion molecule 1; Cy, cyanin; cyt *c*, cytochrome *c*; DC, dendritic cell; ES, enrichment score; GSEA, gene set enrichment analysis; ID2, inhibitor of DNA protein 2; IRF8, IFN regulatory protein 8; LD, low density; L-DC, lymph dendritic cell; LT-DC, lymphoid tissue conventional dendritic cell; pDC, plasmacytoid dendritic cell; qRT-PCR, quantitative RT-PCR.



www.jimmunol.org/cgi/doi/10.4049/jimmunol.1000824

functional specialization for $CD8^+$ T cell activation has been ascribed to non-LT migratory $CD103^+$ DCs in the lung (14), intestine (15), and skin (16–18). Interestingly, most of the non-LT $CD103^+$ DCs, except gut $CD11b^+CD103^+$ DCs, were found to be related to the LT $CD8\alpha^+$ DCs in that they derive from the same precursor in a pathway depending on FLT3 ligand, inhibitor of DNA protein 2 (ID2), and IFN regulatory protein 8 (IRF8) (19, 20). In addition, deletion of the basic leucine zipper transcription factor ATF-like 3 (BATF3) abrogated the development of both the dermal $CD103^+$ DCs and the LT $CD8\alpha^+$ DCs (20, 21).

A main challenge in the DC field is to translate the knowledge on the functional specialization of the murine DC subsets to other species of medical, economical, and environmental importance. This is of prime necessity for the development of new generation of DC-targeted vaccines applicable to mammals, with skin DCs being the direct targets of most vaccines. We have reported that the human blood DC Ag $(BDCA)3^+$ and $BDCA1^+$ DC subsets resemble the mouse spleen $CD8\alpha^+$ and $CD11b^+$ DC subsets, respectively, based on transcriptomic analyses (22). During the process of the review of this article, four other articles, including one from our group, were published that characterize the human blood $BDCA3^+$ DCs as a putative functional equivalent of the murine splenic $CD8\alpha^+$ DCs (23–26).

To attempt to generate a unifying view of DC subset organization with distinct and specific functions that can be generally applied to mammals, we comparatively studied conventional DCs in three distant mammalian species in which DC subsets have been described (i.e., sheep, human, and mouse) and in different tissues. Sheep belong to the Laurasiatheria, a superorder of mammals distinct from the Euarchontoglires that includes humans and rodents (27). These two superorders of eutherian mammals diverged ~90 million years ago (27). In addition, sheep provides the unique opportunity to access migratory DCs originating from skin using pseudo-afferent lymph duct cannulation and renders possible the investigation of DC subset functions in a large mammal species. The sheep lymph DCs (L-DCs) are semimature $CD1b^+$ DCs coexpressing membrane and intracellular MHC class II colocalized with DC lysosome-associated membrane glycoprotein (28, 29). Two subsets have been described in cattle and sheep skin lymph, identified as $CD26^+$ $SIRP\alpha^-$ and $CD26^-SIRP\alpha^+$ L-DCs, that appear to display distinct phenotypes and properties (28, 30). Notably, we have reported previously that sheep $CD26^+SIRP\alpha^-$ L-DCs constitutively transport apoptotic bodies in vivo contrary to their $CD26^-SIRP\alpha^+$ counterparts (28). This suggested that $CD26^+SIRP\alpha^-$ L-DCs may resemble mouse $CD8\alpha^+$ DCs in that they could have a higher ability for capture of apoptotic bodies and subsequent cross-presentation of exogenous Ags derived from dead cells for induction of tolerance to self or immunity to intracellular pathogens. We thus hypothesized that characterizing the functions of sheep L-DC subsets and comparing their gene expression profiling to those of mouse and human DC subsets could help to identify features of DC subset organization that are conserved in species from distant mammal superorders, independently of the tissue of origin.

## Materials and Methods

### *Sheep and surgery*

Prealpes female sheep (between 2 and 4 y old) were raised and housed in the Institut National de la Recherche Agronomique animal experimentation unit in Jouy-en-Josas, France. Skin prescapular pseudo-afferent and cervical efferent lymph duct cannulations were performed in sheep as described previously (31, 32). A total of 17 sheep, including 12 cannulated sheep, were finally used to perform the study. Sheep received 1000 International Units Lovenox (Sanofi-Aventis, Paris, France) s.c. twice per day. Sheep cannulation is technically very demanding with a success rate of ~50%, explaining the limited number of animals used per experiment. Three sheep were vaccinated with 40 mg OVA or with bluetongue virus (BTV) vaccine (BTV serotype 2, provided by Merial, Lyon, France) in CFA below the ear twice at 3 wk intervals before efferent cannulation. All of the animal experiments were conducted under the authority of a license issued by the Direction des Services Vétérinaires of Versailles (accreditation numbers 78-93, 78-15, and A78-730) and with agreement from the Regional Paris South Ethics Committee (number 08-002).

### *Dermal and lymph node cell isolation*

Eight-millimeter skin punches were incubated in 1.44 mg/ml dispase (1.75 U/ml) for 18 h at 4°C and then for 2 h at 37°C. Dermal sheets were separated from the epidermis and placed in RPMI 1640 and 10% FCS for 24 h, and the migrated cells were collected for subsequent labeling. Lymph node fragments were minced and incubated in collagenase (2 mg/ml)/DNase (0.5 mg/ml)/dispase (0.5 mg/ml) for 1 h. Low density (LD) cells were enriched using Optiprep gradient (Nycomed Pharma, Oslo, Norway).

### *L-DC immunolabeling and flow cytometry analyses*

Lymph was collected twice per day and then kept at 4°C. LD lymph cells (25–50% DCs) were obtained after centrifugation on a 1.065 density iodixanol gradient according to procedures described previously by our group (33). They were used either fresh or frozen depending on the number of cells required for the experiments. LD lymph cells were labeled as previously reported (28, 33, 34) using anti-ruminant determinant-reacting mAbs, including anti-CD1b (Th97A, [IgG2a]), anti-CD26 (CC69 [IgG1]), anti-SIRP (ILA24 [IgG1]), anti-CD205 (CC98 [IgG2b]), anti-CD4 (ST4 and 17D1 [IgG1], GC50A1 [IgM]), CD8 (7C2 [IgG2a], CACT80C [IgM]), CD11b (MM12A [IgG1], ILA130 [IgG2a]), CD14 (CAM36A [IgG1]), γ/δ T cells (86D and ILA29 [IgG1]), CD45RB (CC76 [IgG1]), anti-B cells (DU2-104 [IgM]), anti-CD45RA (73B1 [IgG1]), anti-MHC class II (Th14B [IgG2a]), and appropriate isotype control mAbs. For cell adhesion molecule 1 (CADM1) detection, the chicken anti-mouse CAMD1 3D1 mAb followed by FITC-conjugated purified rabbit IgG directed to chicken Ig was used (bovine and mouse CADM1 share 94% amino-acid identity).

### *Selection of L-DC subsets, allogeneic naive $CD4^+$ and $CD8^+$ T cells, and autologous BTV- or OVA-immune $CD8^+$ T cells*

For gene expression studies, thawed LD afferent lymph cells were labeled with anti-CD1b and anti-CD26 followed by fluorochrome-conjugated anti-mouse specific Ig isotype purified goat IgG (Caltag Laboratories, Burlingame, CA), and the subsets were sorted with a fluorescence-activated flow sorter (FACSAria; BD Immunocytometry Systems, San Jose, CA) at a >99% purity level. For functional studies, $CD26^+$ and $CD26^-$ DC subsets were enriched from thawed LD afferent lymph cells using immunomagnetic selection to preserve their viability, because FACS-sorted L-DCs did not survive >12 h in vitro (>85% purity). To deplete T cells, B cells, NK cells, monocytes, and pDCs, thawed LD lymph cells were reacted with a mixture of mAbs including anti-ruminant CD4, CD8, CD11b, CD14, γ/δ T cells, CD45RB, and anti-B cells and subsequently depleted of the labeled cells with anti-mouse IgG and IgM-coated Dynabeads (Dynal Biotech France, Compiègne, France) followed by a mix of immunomagnetic Dynabeads (Dynal) coated with human mAb anti-mouse IgG and rat mAb anti-mouse IgM, according to the manufacturer's recommendations. DCs were further labeled with anti-CD26 mAb followed by magnetic microbeads coated with goat anti-mouse IgG H and L chains (Miltenyi Biotec, Auburn, CA) and positively selected with a MACS LS column and negatively selected with a subsequent MACS CS column. The efficiency of positive and negative selections was examined at each step of the procedure by FACS.

Naive $CD45RA^+CD4^+$ and $CD45RA^+CD8^+$ T cell subsets were selected from the fresh efferent lymph cells of sheep by immunomagnetic sorting (>85% purity). Fresh efferent lymph cells were washed and labeled with anti-CD11b, CD1b, CD14, γ/δ T cells, B, and CD4 mAbs followed by a mix of immunomagnetic Dynabeads. The negative fraction was further labeled with anti-CD45RA mAb, followed by magnetic microbeads coated with goat anti-mouse IgG H and L chains (Miltenyi Biotech) and positively selected with a MACS LS column. The same procedure was done for naive CD4 T cells except that anti-CD8 mAbs were used instead of anti-CD4 mAbs in the mixture. The efficiency of the positive and negative selections was examined by FACS.

The $CD8^+$ T cells from OVA- or BTV-immune sheep were obtained from the cervical efferent lymph of sheep vaccinated with OVA or BTV vaccine in the corresponding lymph anatomical territory. Fifteen days after the boost below the sheep ear, the cervical efferent lymph was collected and the $CD8^+$ T cells were isolated by negative immunomagnetic selection. The purity of the negative fraction was checked by FACS and was >85% for subsequent Ag presentation assays.

### *IL-12p40 and IFN-γ protein detection*

IL-12p40 was detected by ELISA using the anti-ruminant CC326 and CC301 mouse mAbs (Serotec, Oxford, U.K.) following a previously published protocol (35). IFN-γ was detected using the anti-ruminant IFN-γ CC330 and CC302 mAb (Serotec) as described previously (34).

### *Gene expression studies*

Total mRNA from L-DCs (called "reference") and FACS-purified L-DC subsets was extracted using the Qiagen RNeasy Micro Kit (Qiagen, Valencia, CA) and checked for quality on an 2100 Bioanalyzer with RNA 6000 Nano Chip kit (Agilent, Palo Alto, CA). Total RNAs (200 ng) were amplified by linear PCR, and the amplification products were labeled with cyanin (Cy)-3 using the BioPrime Array CGH Genomic Labeling System Kit (Invitrogen, Carlsbad, CA). RNA from the L-DC reference preparation was similarly amplified, labeled by Cy5, and used as a reference probe for the hybridization. Each Cy3-labeled cDNA was cohybridized with the Cy5 reference probe onto ovine 15K 60-mer microarrays (15,208 probes, reference G4813A, AMADID 19921; Agilent) following the manufacturer's protocol. Raw data were extracted from scanned microarray images using Feature Extraction Software version 9.5 (Agilent) and normalized using the Quantile method adapted to bicolor microarrays. All of the protocols used can be obtained by contacting the microarray and sequencing platform of the Institut de Génétique et de Biologie Cellulaire et Moléculaire (www.microarrays.u-strasbg.fr). Two independent biological replicates were performed for each L-DC subset by using cells isolated from two different animals. The microarray data have been assigned the Gene Expression Omnibus number GSE21889 (www.ncbi.nlm.nih.gov/geo), and they are publicly available.

The gene set enrichment analysis (GSEA) method from the Massachusetts Institute of Technology [www.broad.mit.edu/gsea (36)] was used to statistically test whether a set of genes of interest (a GeneSet) was distributed randomly in a larger list of genes sorted according to a given measure (a GeneList). In our study, the GeneLists correspond to all of the genes for which at least one ProbeSet is present on the mouse or human Affymetrix (Santa Clara, CA) chips used, ranked from high expression in mouse $CD8\alpha^+$ or human $BDCA3^+$ DCs to high expression in mouse $CD11b^+$ DCs or human $BDCA1^+$ DCs or mouse/human pDCs. The "$CD26^+$ over $CD26^-$" GeneSet is defined as the list of the genes that are expressed at least 2-fold higher in the $CD26^+$ DCs as compared with the $CD26^-$ DCs independently in both of the sheep used for the microarray analyses and reciprocally for the "$CD26^-$ over $CD26^+$" GeneSet. To establish the $CD26^+$ versus $CD26^-$ sheep GeneSet, the orthologous mouse and human genes and their corresponding Affymetrix ProbeSets were retrieved by batch query of the Ensembl database using the MartView tool of the BioMart software (www.biomart.org). An enrichment score (ES) was calculated, for example, for the "$CD26^+$ over $CD26^-$" GeneSet in mouse $CD8\alpha^+$ versus $CD11b^+$ DC subsets, by walking down the mouse GeneList from the genes highly expressed in $CD8\alpha^+$ DCs to those highly expressed in $CD11b^+$ DCs to determine whether each of the individual genes of the GeneList belongs to the GeneSet. The absolute value of the ES goes up when a gene from the GeneList belongs to the GeneSet whereas it goes down otherwise. If the genes of the GeneSet are not differentially expressed between the two populations, then they will be uniformly distributed in the GeneList and the ES will remain low. If more genes of the GeneSet are expressed to higher levels in the first population, then they will be distributed together in the beginning the GeneList and the ES will steadily increase before getting back to 0. If more genes of the GeneSet are expressed to higher levels in the second population, then they will be distributed together in the end the GeneList and the ES will peak at a negative value. The maximal absolute value that the ES can reach is 1. The higher the absolute value of the ES, the more the GeneSet is enriched in one of the populations studied as compared with the other. In addition, a false discovery rate $q$ value was also calculated that evaluates the probability that a GeneSet called enriched is a false positive. Results were considered significant when this probability was below 10% ($q < 0.1$).

Quantitative real-time PCR was carried out using 5–25 ng cDNA, in duplicate, with 300 nM of each primer and the SYBR Green PCR Master Mix (Applied Biosystems, Foster City, CA). Oligonucleodies were designed using the Primer Express software (version 2.0) with *Ovis aries* ESTs (>400 nt) orthologous to the bovine (>93% nucleotide identity) and human (>79% identity) sequences or with bovine sequences when ovine ESTs were not available (marked with an asterisk). They include GAPDH (forward 5′-CACCATCTTCCAGGAGCGAG-3′, reverse 5′-CCAGCATCACCCCACTTGAT-3′), IL-12p40 (forward 5′-GAATTCTCGGCAGGTGGAAG-3′, reverse 5′-GTGCTCCACGTGTCAGGGTA-3′), IL-10 (forward 5′-TGCTGGATGACTTTAAGGGTT-3′, reverse 5′-TCATTTCCGACAAGGCTTGG-3′), IL-13 (forward 5′-AGAACCAGAAGGTGCCGCT-3′, reverse 5′-GGTTGAGGCTCCACACCATG-3′), IFN-γ (forward 5′-TGATTCAAATTCCGGTGGATG-3′, reverse 5′-TTCATTGATGGCTTTGCGC-3′), TNF-α (forward 5′-CAAGGGCCAGGGTTCTTACC-3′, reverse 5′-GCCCACCCATGTCAAGTTCT-3′), IL-6 (forward 5′-GCTGCTCCTGGTGATGACTTC-3′, reverse 5′-GGTGGTGTCATTTTTGAAATCTTCT-3′), IL-22* (forward 5′-GCAGAAGCCTCGATACAGGTTCT-3′, reverse 5′-GCCATCGTGGACAAAGCAA-3′), CADM1 (forward 5′-CCCCCGCAGGAAAGTTACA-3′, reverse 5′-TGTCTTTCTGGATATCGATCATCAG-3′), Clec9A (forward 5′-GCTATAATGCAGCAGCAAGAAAAA-3′, reverse 5′-GGGTTTCTCTTCCACTGTGAGAA-3′), C1orf21 (forward 5′-GCTGAAGCTGACCGAATGAGA-3′, reverse 5′-TCATTTTGAACAGTGGCAACATG-3′), IRF8 (forward 5′-GGAGTGTGGGCGCTCTGA-3′, reverse 5′-TCACCATCCCCATGTAGTCATC-3′), MIST (forward 5′-TGCTCAGGCTGAGTTGAAGATC-3′, reverse 5′-GCCCGGTCTGTTCATCTTTC-3′), IDO1 (forward 5′-GCCTCCGAGGCCACAAG-3′, reverse 5′-CATACGCCATGGTGATGTATCC-3′), CSF1R (forward 5′-GGTACCCCCAGCCCAATG, reverse 5′-CGTGGGTCTTATCACATCTGTTG-3′), BatF3 (forward 5′-CGAACATGAGCCCTGAGGAT-3′, reverse 5′-CTGAGCAGCAACTCGGTTTTT-3′), ID2 (forward 5′-CAAGAAGGTGAGCAAGATGGAA-3′, reverse 5′-CGCGATCTGCAAGTCCAA-3′), SIRPα (forward 5′-GCCGGCCTGGGAACTG-3′, reverse 5′-CGCGGAGCGTCAAGGA-3′). The primers were all checked for PCR amplification efficiency. PCR cycling conditions were 95°C for 10 min, linked to 40 cycles of 95°C for 15 s and 60°C for 1 min. Real-time PCR data were collected by the 7900HT sequence detection system (Applied Biosystems), and $2^{-\Delta\Delta CT}$ calculations for the relative expression of the different genes (arbitrary units) were performed with SDS 2.1 software (Applied Biosystems) using GAPDH for normalization.

### *Capture of apoptotic bodies by L-DC subsets in vivo*

Allogeneic PBMCs were isolated from blood by Percoll gradient centrifugation as described previously (34). PBMCs ($2 \times 10^8$) were UV-irradiated to induce apoptosis (250 mJ/cm$^2$), labeled with CFSE, and injected intradermally in the skin on the shoulder of a cannulated sheep. The first 3 h lymph collection was eliminated to avoid $CFSE^+$ cells originating from the passive translocation of the injection cell bolus. Eighteen hours postinjection, LD lymph cells were stained for CD1b and CD26 detection and the percentage of $CFSE^+$ cells in $CD26^+$ and $CD26^-$ L-DCs was evaluated by FACS.

### *Endosomal FITC quenching*

Acidification in DC subset endosomes was determined as described previously by us (12). LD cells ($2 \times 10^6$) were incubated with 5 mg/ml FITC-conjugated dextran 40,000 m.w. (pH-sensitive) and FluoProbes 647-conjugated dextran 40,000 m.w. (pH-insensitive) for 10 min at 37°C and then extensively washed in a large volume of cold PBS and 2 mM EDTA (pulse). After being washed, the cells were resuspended in X-VIVO15 medium and 2% FCS and incubated at 37°C (chase) for the indicated times and immediately placed on ice. A control at 4°C during pulse and chase was done to determine FITC and FluoProbes 647 fluorescence positivity. CD1b and CD26 staining was done, and the geometric mean intensities of the $FITC^+$ and FluoProbes $647^+$ $CD26^+$ and $CD26^-$ DCs were established by FACS after a 0, 10, and 20 min chase. The ratio between the two geometric mean fluorescence intensities was calculated, and the quenching rate in each subset was evaluated by the formula: 1 − [FITC/FluoProbes 647 geometric mean ratio in chased cells: FITC/FluoProbes 647 geometric mean ratio in pulsed cells].

### *Sensitivity to cytochrome* c *treatment*

LD lymph cells were cultured with 2–30 mg/ml horse cytochrome *c* (cyt *c*; Sigma-Aldrich, St. Louis, MO) in X-VIVO15 medium (BioWhittaker, Walkersville, MD) and 2% FCS, 100 IU/ml penicillin, and 100 μg/ml streptomycin (complete medium). After overnight culture at 37°C, cells were labeled with anti-CD1b, CD26, and SIRPα mAbs and PE-conjugated annexin V (Caltag Laboratories) and were analyzed by FACS.

### *T cell activations*

For MLR, total L-DCs and selected $CD26^+$ and $CD26^-$ L-DCs ($5 \times 10^4$) were plated with allogeneic CSFE-labeled naive CD4 or CD8 T cells ($5 \times 10^5$) in 200 μl complete medium. After 5 d, live cells were identified by 7-aminoactinomycin D exclusion and the percentage of divided living T cells was monitored by reduction of CFSE labeling.

For OVA presentation, total L-DCs and selected $CD26^+$ and $CD26^-$ L-DCs ($5 \times 10^4$) were incubated overnight with 500 μg/ml OVA. For BTV Ag stimulation, DCs were infected overnight with culture-adapted BTV

serotype 2-infected baby hamster kidney (BHK) cells or with uninfected BHK cells (three BHK cells for one DC) that had been UV-irradiated for to 2 min to prevent cell division but not viral infectivity. The next day, OVA- or BTV serotype 2-immune autologous $CD8^+$ T cells ($5 \times 10^5$) were added to the wells. After 3 d, supernatants were harvested for IFN-γ detection.

### *Statistical analysis*

Statistical significance of functional tests was estimated with a paired Student *t* test. For the GSEAs, the significance threshold recommended by the software developers is a false discovery rate below 25% ($q < 0.25$), which constitutes a more stringent requirement than if based on the nominal *p* value [www.broadinstitute.org/gsea/doc/GSEAUserGuideFrame.html (36)]. We have chosen $q < 0.1$ for even higher stringency.

## Results

### *Sheep $CD26^+$ and $CD26^-$ skin L-DCs are distinct DC subsets as revealed by their genome-wide expression profiling*

The sheep L-DCs comprise two subsets distinguished by their differential expression of CD26 and SIRPα (i.e., $CD26^+SIRP\alpha^-$ and $CD26^-SIRP\alpha^+$ cells) (Fig. 1) (28). The $CD26^+$ L-DCs constitute $14.4 \pm 2.5\%$ of the total skin migrating L-DCs (28). In addition, we show that these two DC subsets are detected in skin and in lymph nodes in similar proportions as those in lymph (Fig. 1). Sheep L-DCs do not express CD8α nor CD11b, and they do not react with Abs to human BDCA3 or BDCA1 (data not shown), but they share with mouse $CD8\alpha^+$ DCs the cytosolic presence of apoptotic bodies (28) and the low expression of SIRPα (37). Thus, to determine to what extent sheep L-DC subsets resemble known mouse spleen and/or human blood DC subsets and whether a common signature can emerge, we performed a wide comparative gene expression profiling of these different cell populations. Specifically, we took advantage of the recent availability of pangenomic ovine microarrays to examine the global gene expression program from FACS-sorted $CD26^+$ and $CD26^-$ L-DCs from two sheep (#81 and #66) and to compare it to that of mouse spleen and human blood DCs. Overall 750 probes were consistently expressed differentially in both sheep between $CD26^+$ and $CD26^-$ skin L-DCs, with 365 probes expressed to higher levels in $CD26^+$ L-DCs (referred to as the $CD26^+$ GeneSet) and 385 in their $CD26^-$ counterparts (referred to as the $CD26^-$ GeneSet). Thus, there is a strong difference in the gene expression profiles from sheep $CD26^+$ and $CD26^-$ skin L-DCs, suggesting that these cells correspond to distinct DC subsets.

To further delineate how biologically important the differences in the gene expression programs from sheep $CD26^+$ and $CD26^-$ skin L-DCs could be, we next examined the $CD26^+$ versus $CD26^-$ GeneSets for clues toward major differences that could exist in the ontogeny or the functions of these cell types. To this aim, we retrieved the mouse and human gene orthologues to the genes constituting the sheep $CD26^+$ versus $CD26^-$ GeneSets, and we examined whether the corresponding human or mouse gene lists were enriched for specific annotation terms using the DAVID Gene Ontology mining tool (38). Specific terms were retrieved for both subsets of DCs, suggesting that they could indeed develop under the instruction of different molecular signals and be involved in different functions. For example, the gene signature of $CD26^-$ L-DCs was significantly enriched in genes involved in cellular lipid metabolic processes, fatty acid metabolic processes, inflammatory responses, and hydrolase or protease activity (Supplemental Table I). This population was also characterized by the expression of a specific set of C-type lectin receptors or associated signaling adaptors, CLEC3B, CLEC4E, CLEC6A, FCER2, and ASGR2, and by high expression of the growth factor receptor CSF1R. The gene signature of sheep skin $CD26^+$ L-DCs was significantly enriched for genes involved in Ag processing and presentation, the TLR signaling pathway, cell adhesion, or hematopoiesis (Supplemental Table II). Several of the genes enriched in sheep skin $CD26^+$ L-DCs correspond to orthologues of mouse genes known to be specifically involved in the development or the functions of mouse $CD8\alpha^+$ DCs as recently reviewed (3) including the transcription factors ID2, IRF8, BATF3, the enzyme IDO1, the membrane markers CLEC9A and CADM1, and the cytokine IL-12 (Figs. 2, 3, Table I). Most of these genes are also overexpressed by human $BDCA3^+$ DCs (Table I). Therefore, this genome-wide expression suggests that sheep skin $CD26^+$ L-DCs may share major genetic characteristics in common with mouse $CD8\alpha^+$ and human $BDCA3^+$ DCs.

### *Sheep skin $CD26^+/CD26^-$ L-DCs, mouse lymphoid organ $CD8\alpha^+/CD11b^+$ DCs, and human blood $BDCA3^+/BDCA1^+$ DCs share significant transcriptomic similarities across species*

To perform a global and unbiased comparison of the gene expression programs of sheep skin $CD26^+$ and $CD26^-$ L-DC subsets, human blood $BDCA3^+$ and $BDCA1^+$ DC subsets, and mouse spleen $CD8\alpha^+$ and $CD11b^+$ DC subsets, we performed an analysis with GSEA. The GSEA results are included in Table II, and they are represented graphically as enrichment plots in Supplemental Figs. 1 and 2. The GSEA approach clearly demonstrated that a significant number of the genes selectively expressed to high levels in sheep skin $CD26^+$ L-DCs were also expressed to higher levels in human blood $BDCA3^+$ DCs ($q < 10^{-3}$, with 16 genes >2-fold higher in $BDCA3^+$ DCs versus 3 genes >2-fold higher in $BDCA1^+$ DCs; Supplemental Fig. 1, Table II) or in mouse spleen $CD8\alpha^+$ DCs ($q = 0.01$, with 24 genes >2-fold higher in $CD8\alpha^+$ DCs versus 14 genes >2-fold higher in $CD11b^+$ DCs; Supplemental Fig. 2, Table II). Conversely, the sheep $CD26^-$ GeneSet was enriched in human blood $BDCA1^+$ DCs ($q < 10^{-3}$, with 23 genes >2-fold higher in $BDCA1^+$ DCs versus 6 genes >2-fold higher in $BDCA3^+$ DCs) or in mouse spleen $CD11b^+$ DCs ($q = 0.08$, with 17 genes >2-fold higher in $CD11b^+$ DCs versus 9 genes >2-fold higher in $CD8\alpha^+$ DCs). As a control, the GeneSets were examined for differential enrichment between pDCs and $CD8\alpha^+$, $CD11b^+$, $BDCA3^+$, or $BDCA1^+$ DCs. No significant enrichment of the GeneSets was observed in pDCs (Supplemental Figs. 1, 2, Table II). For example, when comparing human pDCs and $BDCA1^+$ DCs, the

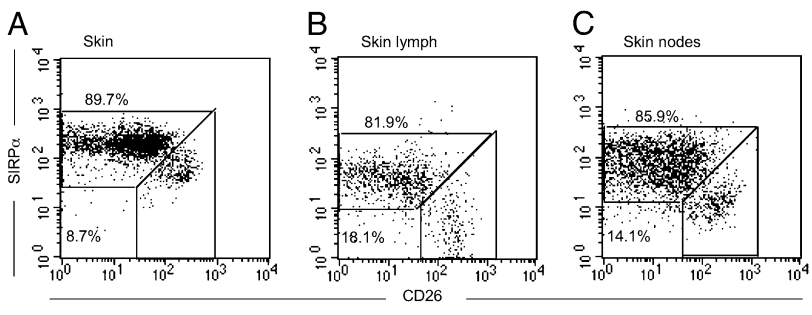


**FIGURE 1.** CD26 and SIRPα expression defines two L-DC subsets and are found in skin and in skin draining lymph nodes. *A*, Skin was labeled with anti-MHC class II, anti-CD26, and anti-SIRPα mAbs; the MHC class $II^{high}$ cells were selected with appropriate gating and analyzed for CD26 and SIRPα expression. *B* and *C*, LD lymph and lymph node cells were labeled with anti-CD1b, CD26, and SIRPα mAbs; the $CD1b^+$ cells were selected with appropriate gating and analyzed for CD26 and SIRPα expression.

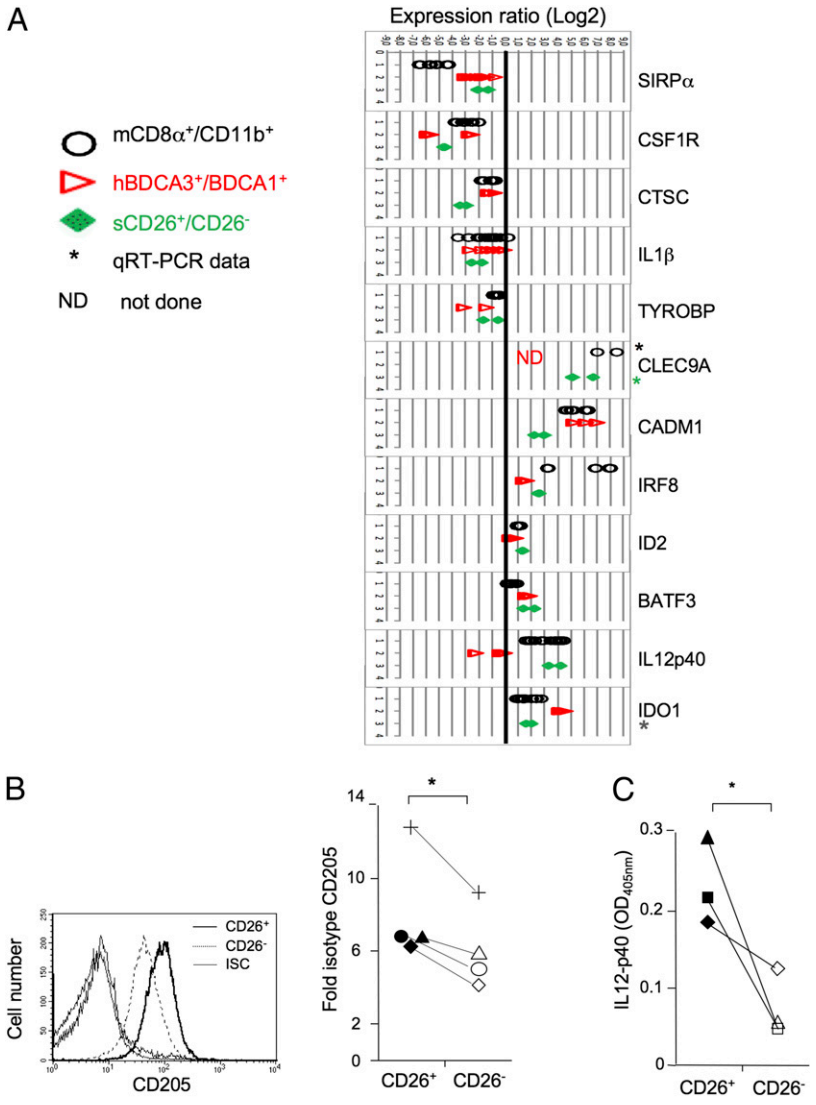


**FIGURE 2.** Genes and protein expression in mouse lymphoid organ CD8α$^+$/CD11b$^+$, human blood BDCA3$^+$/BDCA1$^+$, and sheep lymph CD26$^+$/CD26$^-$ DC subsets. *A*, Comparison of the expression of selected genes in mouse, human, and sheep DCs. The expression ratios (*x*-axis, in $Log_2$) of selected representative genes were compared between mouse spleen CD8α$^+$ and CD11b$^+$ (black dots), human blood BDCA3$^+$ and BDCA1$^+$ (red triangles), and sheep lymph CD26$^+$ and CD26$^-$ (green diamonds) DC subsets. The data illustrated were obtained by microarray analysis, except for CLEC9A (sheep and mouse) and IDO1 (sheep), the expression of which was evaluated by qRT-PCR because these genes were not represented among the probes on the corresponding microarrays. *B*, Fold isotype mean fluorescence intensity of CD205 staining of sheep lymph CD1b$^+$CD26$^+$ and CD1b$^+$CD26$^-$ L-DCs as measured by FACS (four different sheep). *C*, Detection of IL-12p40 protein secretion by immunomagnetically selected CD26$^+$ and CD26$^-$ L-DCs (OD at 405 nm in ELISA, three different sheep). For *A* and *C*, significance of the differences was calculated with a paired *t* test ($*p < 0.05$). Sheep L-DCs: +, #81; ●, #55; ■, #66; ◆, #33; ▲, #70.

CD26$^-$ GeneSet was enriched in the BDCA1$^+$ DCs as expected, whereas the BDCA3$^+$ GeneSet also showed a trend toward enrichment in the BDCA1$^+$ DCs and not in the pDCs that did not reach significance. The only pairwise comparisons of DC subsets where the CD26$^+$ and CD26$^-$ GeneSets were significantly enriched in reciprocal populations were those comparing human BDCA3$^+$ and BDCA1$^+$ DC subsets on the one hand or mouse CD8α$^+$ and CD11b$^+$ DC subsets on the other hand. Eleven genes found to be differentially expressed between mouse CD8α$^+$/CD11b$^+$, human BDCA3$^+$/BDCA1$^+$ DC, and sheep CD26$^+$/CD26$^-$ L-DCs in microarrays were analyzed by quantitative RT-PCR (qRT-PCR) and their expression profile was confirmed (IRF8, IL-12p40, MIST, BATF3, ID2, C1orf21, TNF-α, IL-6, CSF1R, SIRPα, and CADM1) (Figs. 2, 3). In addition, we also extended these results to two genes, IDO1 and CLEC9A, that are known to be specifically expressed in mouse CD8α$^+$ and human BDCA3$^+$ DCs as compared with their DC counterparts (3, 10, 39) and for which ProbeSets were not identified on the ovine microarray by demonstrating their specific expression in sheep CD26$^+$ L-DCs using qRT-PCR (Figs. 2, 3). Finally, at the protein level on sheep L-DCs, we also found that surface CD205 and secreted IL-12p40 were more expressed by CD26$^+$ L-DCs than by CD26$^-$ L-DCs, as is the case for mouse CD8α$^+$ DCs versus CD11b$^+$ DCs ($p < 0.05$; Fig. 2*B*, 2*C*) (40, 41).

Thus, on the basis of their global gene expression program, sheep skin CD26$^+$ L-DCs resemble mouse spleen CD8α$^+$ DCs and human blood BDCA3$^+$ DCs, whereas sheep skin CD26$^-$ L-DCs resemble mouse spleen CD11b$^+$ DCs and human blood BDCA1$^+$ DCs. Of note, human BDCA3$^+$ DCs express more surface CD26 protein than pDCs and BDCA1$^+$ DCs, suggesting that the sheep DC subset distinction based on CD26 and SIRPα expression applies to human BDCA3$^+$ DCs (Fig. 4).

### *Sheep CD26$^+$ skin L-DCs are more efficient than their CD26$^-$ counterparts for the activation of allogeneic naive CD8 T cells*

To evaluate whether the differential transcriptomic profiles between sheep CD26$^+$ and CD26$^-$ L-DCs would translate into differential capacities to activate naive T cells, we performed allogeneic MLR. These experiments required that we isolate naive CD4$^+$ and CD8$^+$ T cells from fresh efferent sheep lymph, which is a more manageable source of naive T cells as compared with blood in this species (42). In three independent experiments, CD26$^+$ L-DCs were found to be more potent than CD26$^-$ L-DCs to stimulate the division of naive CD8$^+$ T cells ($p < 0.05$; Fig. 5*A*, Supplemental Fig. 3*A*). We also examined the capacity of the L-DC subsets to induce the expression of cytokine genes, because most cytokines cannot be detected at the protein level in sheep. In CD8$^+$ T cell/L-DC subset MLR, IFN-γ mRNA was found to be expressed at higher levels in the cocultures with CD26$^+$ L-DCs than with the CD26$^-$ L-DCs (Fig. 5*B*). Thus, sheep CD26$^+$ skin L-DCs are more efficient than

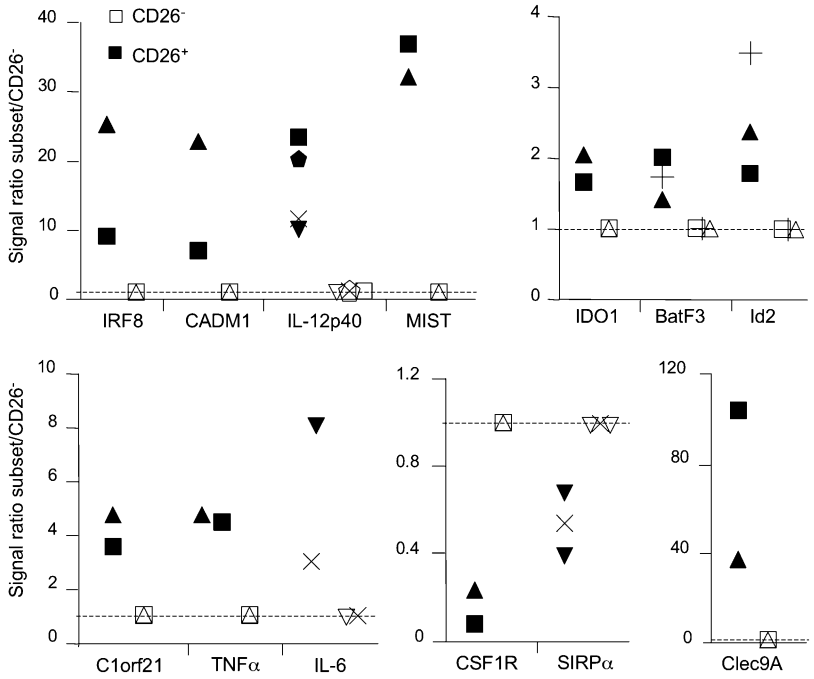


**FIGURE 3.** Expression of selected molecules in $CD26^+$ and $CD26^-$ L-DCs. The expression of selected genes in the L-DC subsets purified from different sheep was analyzed by qRT-PCR and was normalized with GAPDH (see *Materials and Methods* section for primer sequences). Relative expression ratios were calculated for each gene in $CD26^+CD1b^+$ versus $CD26^-$ $CD1b^+$ L-DCs. Sheep L-DCs: +, #81; ●, #55; ■, #66; ♦, #33; ▲, #70; ▼, #64; ×, #80; pentagon, #31.

their $CD26^-$ counterparts for the activation of allogeneic naive $CD8^+$ T cells.

In addition, $CD26^+$ L-DCs were more efficient than the $CD26^-$ L-DCs for stimulation of the proliferation of naive $CD4^+$ T cells in two out of the three MLR experiments (Fig. 5*A*, Supplemental Fig. 3*B*). However, $CD4^+$ T cell IFN-γ and IL-13 mRNA expression did not consistently appear to be differentially activated by the two L-DC subsets (Fig. 5*B*). Thus, depending on the assays, sheep $CD26^+$ skin L-DCs appear as efficient as, or slightly better than, their $CD26^-$ counterparts for the activation of allogeneic naive $CD4^+$ T cells.

### *Sheep $CD26^+$ L-DCs selectively express high levels of CADM1 in relation to their specific ability to induce* Il22 *gene expression in MLR*

We confirmed by FACS staining that sheep $CD26^+$ L-DCs specifically express high levels of CADM1 as compared with their $CD26^-$ counterparts (Fig. 5*C*). CADM1 has been shown to promote expression of IL-22 mRNA in mouse $CD8^+$ T cells when cultured with APCs engineered to express high surface levels of the CADM1 type 1 lectin (43). CRTAM, the receptor for CADM1, has also been shown to promote IL-22 expression by $CD4^+$ and $CD8^+$ T cells (44). Therefore, we also investigated the expression of IL-22 mRNA in the T cell/L-DC subset MLR (Fig. 5*B*). Strikingly, $CD26^+$ L-DCs were consistently more potent than the $CD26^-$ L-DCs for stimulation of IL-22 mRNA synthesis in naive T cell MLR. IL-22 mRNA was not detected in DC subsets alone, and sorting of $CD4^+$ T cells after a 48 h coculture with L-DCs showed that IL-22 mRNA was induced in the $CD4^+$ T fraction (data not shown). Thus, $CD26^+$ L-DCs selectively induce the expression of the *Il22* gene in $CD8^+$ and $CD4^+$ T cell MLR, which is consistent with their selective expression of CADM1.

### *$CD26^+$ L-DCs are more potent than $CD26^-$ L-DCs for stimulation of autologous OVA-specific $CD8^+$ T cells*

The cardinal property of the mouse $CD8\alpha^+$ DCs is the capacity for cross-priming $CD8^+$ T cells against endocytosed Ags. We thus compared the capacities of sheep $CD26^+$ and $CD26^-$ L-DCs exposed to extracellular soluble OVA for Ag-specific activation of $CD8^+$ T cells. Fig. 6 shows that higher IFN-γ amounts were produced by OVA-specific $CD8^+$ T cells stimulated by autologous OVA-pulsed $CD26^+$ L-DCs as compared with those stimulated by $CD26^-$ L-DCs. However, upon their infection with BTV (33), $CD26^+$ and $CD26^-$ L-DCs similarly activated BTV-specific $CD8^+$ T cells for IFN-γ secretion, indicating that these subsets are equally efficient at stimulating virus-specific $CD8^+$ T lymphocytes when they are directly infected (Supplemental Fig. 4). Overall, our results indicate that the $CD26^+$ L-DCs are superior to the $CD26^-$ L-DCs for activation of an Ag-specific $CD8^+$ T cell response via presentation of exogenous soluble Ag, further demonstrating a common property with the mouse LT $CD8\alpha^+$ DCs.

### *Expression of specific features involved in the cross-presentation pathways is dominantly found in $CD26^+$ L-DCs*

In mouse and human DCs, the cross-priming capacity is strongly associated with a specific regulation of phagosomal and endosomal pH (12). Phagosomal pH was not testable in L-DCs, because sheep L-DCs could not capture 1-μm pH-sensitive FITC-latex beads (data not shown), probably due to their semimature state. We thus tested the differential capacities of $CD26^+$ and $CD26^-$ L-DCs to acidify endosomes using FITC-dextran 40,000 in vitro. Both $CD26^+$ and $CD26^-$ L-DCs incorporated FITC-dextran and the pH-insensitive FluoProbes 647-conjugated dextran with similar efficacies (~10% of positive DCs at 10 min pulse). As shown in Fig. 7*A*, after a 20-min chase, the FITC signal extinction was more pronounced in the $CD26^-$ L-DCs than that in the $CD26^+$ L-DCs ($p < 0.002$). The lower FITC extinction in $CD26^+$ L-DCs indicates that their endosomal pH is more basic than that of $CD26^-$ L-DCs, likewise for mouse $CD8\alpha^+$ DCs as compared with $CD11b^+$ DCs.

Another property associated with cross-priming is the capacity of the DCs to shuffle Ags from the endo-/phagosomal compartment to the cytosol (13, 45). This process of cytosolic diversion can be assessed by a relatively simple assay using as a surrogate parameter the measurement of apoptosis induction in response to exposure to cyt *c*. Indeed, exogenous cyt *c* can induce apoptosis in cells only if it can gain the cytosol after endocytosis to bind apoptotic peptidase activating factor 1 on the outer mitochondrial membrane. After an

Table I. *Genes with conserved selective expression between DC subsets across sheep, mouse, and human*

| Gene Symbol | Gene Title | s_ratio[a] | m_ratio[b] | h_ratio[c] | min ratio[d] |
|---|---|---|---|---|---|
| Genes with higher expression in sheep CD26+, mouse CD8α+, and human BDCA3+ DCs | | | | | |
| XCR1 | Chemokine (C motif) receptor 1 | 8.7 | 41.1 | 32.8 | 8.7 |
| CADM1 | Cell adhesion molecule 1 | 4.7 | 40.8 | 37.1 | 4.7 |
| IRF8 | IFN regulatory factor 8 | 5.7 | 11.0 | 2.4 | 2.4 |
| CPNE3 | Copine III | 3.2 | 2.2 | 5.5 | 2.2 |
| ZDHHC23 | Zinc finger, DHHC domain containing 23 | 2.1 | 2.3 | 1.7 | 1.7 |
| NET1 | Neuroepithelial cell transforming gene 1 | 4.7 | 2.8 | 1.7 | 1.7 |
| AK3 | Adenylate kinase 3 | 2.2 | 1.5 | 5.2 | 1.5 |
| SLAMF8 | SLAM family member 8 | 5.0 | 1.4 | 2.1 | 1.4 |
| GNB4 | Guanine nucleotide binding protein, β4 | 2.4 | 2.4 | 1.3 | 1.3 |
| ID2 | Inhibitor of DNA binding 2 | 2.5 | 2.1 | 1.3 | 1.3 |
| AP1GBP1 | AP1 γ subunit binding protein 1 | 2.1 | 2.0 | 1.2 | 1.2 |
| AP1S3 | Adaptor-related protein complex AP-1, σ3 | 2.7 | 1.6 | 1.2 | 1.2 |
| MAP4K4 | MAPK kinase kinase kinase 4 | 2.3 | 2.2 | 1.1 | 1.1 |
| COL4A3BP | Procollagen, type IV, α3 (Goodpasture Ag) binding protein | 2.3 | 1.1 | 1.4 | 1.1 |
| OSBPL3 | Oxysterol binding protein-like 3 | 2.4 | 2.4 | 1.1 | 1.1 |
| CXCL9 | Chemokine (CXC motif) ligand 9 | 5.7 | 7.5 | 1.0 | 1.0 |
| YWHAZ | Tyrosine 3-monooxygenase/tryptophan 5-monooxygenase activation protein, ζ polypeptide | 2.9 | 1.2 | 1.0 | 1.0 |
| ANPEP | Alanyl (membrane) aminopeptidase | 3.3 | 1.0 | 3.4 | 1.0 |
| Genes with higher expression in sheep CD26−, mouse CD11b+, and human BDCA1+ DCs | | | | | |
| CSF1R | CSF1 receptor | 23.8 | 4.0 | 5.5 | 4.0 |
| SIRPA | Signal regulatory protein α | 4.0 | 19.5 | 6.4 | 4.0 |
| RIN2 | Ras and Rab interactor 2 | 3.1 | 3.4 | 5.4 | 3.1 |
| CTSC | Cathepsin C | 7.8 | 2.1 | 1.8 | 1.8 |
| IL1RN | IL-1R antagonist | 2.5 | 1.8 | 6.9 | 1.8 |
| MALT1 | Mucosa-associated lymphoid tissue lymphoma translocation gene 1 | 2.1 | 2.0 | 1.6 | 1.6 |
| LACTB | Lactamase, β | 5.0 | 1.4 | 1.9 | 1.4 |
| TRAF3 | TNFR-associated factor 3 | 3.0 | 1.6 | 1.3 | 1.3 |
| ZDHHC6 | Zinc finger, DHHC domain containing 6 | 2.6 | 1.3 | 1.3 | 1.3 |
| DBP | D site albumin promoter binding protein | 2.0 | 2.8 | 1.2 | 1.2 |
| SNX11 | Sorting nexin 11 | 2.4 | 1.2 | 1.2 | 1.2 |
| DHRS3 | Dehydrogenase/reductase (SDR family) member 3 | 3.3 | 1.6 | 1.1 | 1.1 |
| CASP4 | Caspase 4, apoptosis-related cysteine peptidase | 2.5 | 1.0 | 2.8 | 1.0 |
| LRRC33 | Leucine-rich repeat containing 33 | 2.1 | 1.9 | 0.9 | 0.9 |
| IL1B | IL-1β | 3.5 | 0.9 | 1.5 | 0.9 |
| SLC40A1 | Solute carrier family 40 (iron-regulated transporter), member 1 | 2.2 | 0.8 | 1.7 | 0.8 |
| NR1H3 | Nuclear receptor subfamily 1, group H, member 3 | 3.0 | 0.8 | 1.2 | 0.8 |

[a] $sCD26^+/sCD26^-$ (first list) or $sCD26^-/sCD26^+$ (second list).
[b] $mCD8\alpha^+/mCD11b^+$ or $mCD11b^+/mCD8\alpha^+$.
[c] $hBDCA3^+/hBDCA1^+$ or $hBDCA1^+/hBDCA3^+$.
[d] Minimal values of the three ratios (sheep, mouse, and human) calculated for each gene.

overnight in vitro culture, cyt *c* induced more annexin $V^+$ DCs within the $CD26^+$ L-DCs as compared with control cultures. In contrast, cyt *c* was not toxic to the $CD26^-$ L-DCs at all of the concentrations tested ($p < 0.05$ at 2 and 5 mg/ml, $p < 0.001$ at 10 mg/ml) (Fig. 7*B*).

Finally, the transportation of apoptotic debris in $CD26^+$ L-DCs (28) suggested a possible functional similarity with the mouse $CD8\alpha^+$ DCs that dominantly capture dead cell bodies for the subsequent cross-priming of $CD8^+$ T cells (9, 45). In addition, $CD26^+$ L-DCs also overexpress *CLEC9A* mRNA (Figs. 2*A*, 3), a C-type lectin expressed on mouse $CD8\alpha^+$ DCs that is mandatory for subsequent cross-presentation of Ags captured from dead cells (11). We thus tested whether the $CD26^+$ L-DCs were indeed more capable than the $CD26^-$ L-DC for capturing dead cells in vivo

Table II. *Results of GSEA analyses*

| | | GeneSets | | | | | | | |
|---|---|---|---|---|---|---|---|---|---|
| | | $CD26^+$ over $CD26^-$ | | | | $CD26^-$ over $CD26^+$ | | | |
| Species | Comparison between DC Subsets | Enriched in[a] | ES[b] | $q$[c] | $n$ Genes[d] | Enriched in[a] | ES[b] | $q$[c] | $n$ Genes[d] |
| Human | $BDCA3^+$ DCs versus $BDCA1^+$ DCs | **$BDCA3^+$** | **0.41** | **$<10^{-3}$** | **16** versus 3 | **$BDCA1^+$** | **0.50** | **$<10^{-3}$** | 6 versus **23** |
| | $BDCA1^+$ DCs versus pDCs | $BDCA1^+$ | 0.30 | 0.195 | 24 versus 21 | **$BDCA1^+$** | **0.42** | **0.001** | **34** versus 11 |
| | $BDCA3^+$ DCs versus pDCs | **$BDCA3^+$** | **0.40** | **0.006** | **26** versus 24 | pDCs | 0.27 | 0.461 | 24 versus 18 |
| Mouse | $CD8\alpha^+$ DCs versus $CD11b^+$ DCs | **$CD8\alpha^+$** | **0.34** | **0.012** | **24** versus 14 | **$CD11b^+$** | **0.32** | **0.082** | 9 versus **17** |
| | $CD11b^+$ DCs versus pDCs | **$CD11b^+$** | **0.47** | **$<10^{-3}$** | **35** versus 16 | **$CD11b^+$** | **0.37** | **0.038** | **20** versus 13 |
| | $CD8\alpha^+$ DCs versus pDCs | **$CD8\alpha^+$** | **0.50** | **$<10^{-3}$** | **39** versus 14 | **$CD8\alpha^+$** | **0.33** | **0.071** | **19** versus 13 |

[a] The cell population in which the GeneSet is enriched. The population is shown in bold when the enrichment is significant.
[b] The degree to which the GeneSet is overrepresented in the corresponding population. The maximal ES is 1.
[c] $q$, false discovery rate (i.e., the probability that a GeneSet called enriched is a false positive). Results for which $q \leq 0.1$ are considered significant and shown in bold.
[d] Number of genes differentially expressed at least 2-fold between the two populations studied (up in left population versus up in right population).

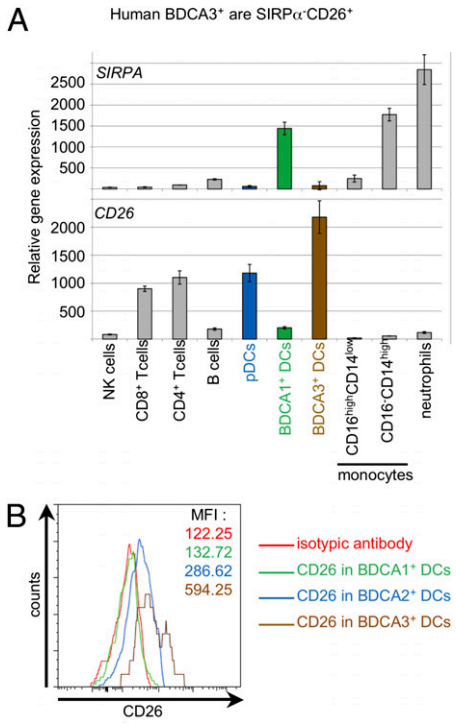


**FIGURE 4.** Human BDCA3$^+$ blood DCs are SIRPα$^-$CD26$^+$. *A*, Expression of the mRNA for CD26 and SIRPα in different leukocyte subsets. The origin and analysis of the microarray data for human leukocyte subsets have been described previously (22). *B*, Expression of CD26 on human blood DC subsets. PBMCs were isolated by Ficoll-Hypaque density gradient centrifugation (Amersham Biosciences, Uppsala, Sweden) from whole-blood samples obtained from normal healthy volunteer donors through the Etablissement Français du Sang according to the French ethics committee on human experimentations. PBMCs were stained with FITC-conjugated anti-CD3, CD14, CD19, or CD20 (lin3; Miltenyi Biotec), allophycocyanin-conjugated anti-CD141 (BDCA3), CD1c (BDCA1), or CD303 (BDCA2) (Miltenyi Biotec), PE-conjugated anti-CD26 (M-A261; BD Biosciences), or isotype control (MOPC-21; BD Biosciences) and LIVE/DEAD Fixable Aqua Dead Cell Stain Kit (Invitrogen) for exclusion of dead cells. The staining for CD26 as compared with that of the isotype control was then examined in the gates for BDCA3$^+$ DCs (lin3$^-$CD141$^+$ live cells), BDCA1$^+$ DCs (lin3$^-$CD1c$^+$ live cells), and BDCA2$^+$ DCs (lin3$^-$CD303$^+$ live cells, pDCs) and is shown as a histogram overlay

by injecting a large quantity of CFSE-labeled apoptotic PBMCs. A low level of CFSE$^+$ DCs could be detected in the collected DCs after 24 h (from 0.05 to 0.55%) (Fig. 8). Notably, the percentage of CFSE$^+$ DCs was constantly higher in the CD26$^+$ DCs versus the CD26$^-$ DCs of the same inoculated sheep ($p < 0.05$) (Fig. 8). Thus, similarly to the mouse CD8α$^+$ DC subset, the CD26$^+$ L-DCs demonstrate a predominant capacity to accumulate CFSE$^+$ apoptotic bodies after in vivo administration.

Altogether, we showed that the CD26$^+$ L-DCs share with the CD8α$^+$ mouse DCs several functional properties that are known to be involved in the exquisite ability of the latter to cross-present exogenous Ags (Table III).

## Discussion

This work shows that the heterogeneity of the DC population follows a conserved organization in phylogenetically distant mammals and different tissues, with correspondence between mouse spleen CD8α$^+$/CD11b$^+$ DCs, human blood BDCA3$^+$/BDCA1$^+$ DCs, and sheep skin CD26$^+$/CD26$^-$ L-DCs. The common transcriptomic profile that we observed allowed us to propose a unifying view on DC subset phenotype across mammal species, with CD8α-like DCs being SIRP$^{lo}$, CADM1$^{hi}$, and DEC205$^{hi}$ and—at least at the RNA level—CLEC9A$^{hi}$ and XCR1$^{hi}$ (Table I). Another originality of our study was to take advantage of the unique ability to collect afferent lymph in sheep to study DC subsets at the migratory stage from the skin to the lymph nodes. This indicates that a similar DC subset dichotomy is found in mammals at different stages of DC migration, maturation, and tissue homing. Furthermore, we provide evidence for a functional specialization of the sheep CD26$^+$ L-DCs. Thus, the results shown here combined with those of the recent functional studies performed on human BDCA3$^+$ DCs (23–26) demonstrate that the sheep skin CD26$^+$ L-DC, the mouse CD8α$^+$ DC, and the human BDCA3$^+$ DC subsets share a high efficiency for the activation of CD8$^+$ T cells against extracellular Ags. Moreover, we show here that sheep skin CD26$^+$ L-DCs share several features known to be characteristic of molecular pathways involved in cross-presentation in mouse CD8α$^+$ DCs. Importantly, consistent with their selective expression of CADM1, the sheep CD26$^+$ L-DCs selectively induce in naive T cells the expression of the *Il22* gene, which encodes a cytokine associated with skin homeostasis and inflammation (46).

Our genome-wide approach was based on the comparison between our microarray data from sheep CD26$^+$ and CD26$^-$ L-DCs and publicly available microarray data from mouse lymphoid organ-resident CD8α$^+$ and CD11b$^+$ DCs and human blood BDCA3$^+$ and BDCA1$^+$ DCs (3, 22). It is striking to observe transcriptomic similarities between pairs of DC subsets originating not only from different species but also from different tissues. In the mouse, the non-LT CD103$^+$ DCs share developmental, phenotypic, and functional similarities with the lymphoid organ-resident CD8α$^+$ DCs (19, 20). It is thus possible that CD26$^+$ L-DCs are equivalent to the mouse dermal CD103$^+$ DCs. This cannot be fully assessed currently, because no transcriptomic data are available yet for mouse dermal CD103$^+$ DCs and may be very difficult to generate due to the rarity of this cell subset [~5% of the mouse dermal DCs (47)]. However, the higher expression of ID2 and IRF8 in sheep CD26$^+$ L-DCs and the higher expression of CSF1R in CD26$^-$ L-DCs are striking observations. Indeed, these molecules are also differentially expressed between non-LT CD103$^+$ DCs and CD103$^-$ DCs in the mouse, and they are key factors in the respective development of these cell types (19). Although transcriptomic similarities were found in our study independently of the tissue origin, it is likely that anatomical localization also strongly impacts the global gene expression profiles of the DC subsets. Indeed, the differences in the gene expression programs of human BDCA3$^+$ versus BDCA1$^+$ DCs were higher when examining cells isolated from tonsils as compared with those isolated from blood (48), presumably due to local activation of the cells in tonsils subsequent to the exposure of Ags or pathogens. Thus, some differences between CD26$^+$ and CD26$^-$ L-DC transcriptomic profiles may be affected by the skin tissue, which is also exposed to the microbial environment in conventional breeding conditions. Nonetheless, our data show that transcriptomic differences between DC subsets in sheep, mouse, and human appear to emerge "above" the tissue microenvironmental influences and pertain to skin, a major site for vaccination and exposure to pathogens.

Some of the genes specifically expressed at higher levels by sheep CD26$^+$ L-DCs as compared with CD26$^-$ L-DCs showed a reciprocal expression pattern between mouse and human DC subsets. CD36 is well known to be expressed at higher levels by mouse CD8α$^+$ DCs (49, 50). It may contribute to their exquisite ability to engulf apoptotic bodies (51), although it is not required for cross-presentation (49, 50). However, on the contrary, CD36 is expressed at higher levels by sheep CD26$^-$ and human BDCA1$^+$ DCs. Similarly, although they are used as bona fide markers for

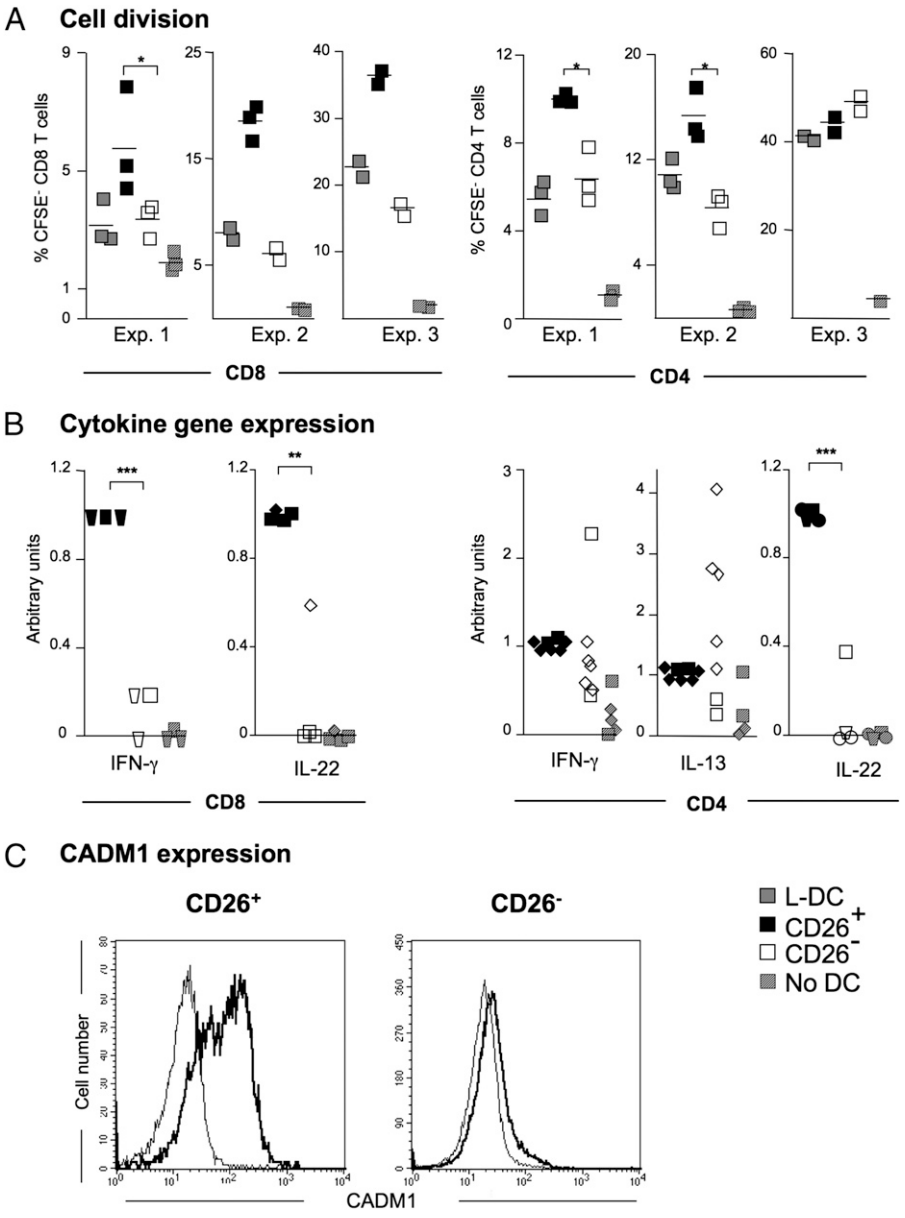


**FIGURE 5.** CD26$^+$ L-DCs are superior to CD26$^-$ L-DCs for activation of CD8$^+$ T cell responses and induction of IL-22 mRNA synthesis in cocultures with naive CD4$^+$ and CD8$^+$ T cells. Immunomagnetically selected L-DCs (gray), CD26$^+$ L-DCs (black), and CD26$^-$ L-DCs (white) (>85% purity, $5 \times 10^4$) were cocultured with allogeneic naive CD4$^+$ or CD8$^+$ T cells (>85% purity, $5 \times 10^5$). *A*, After culture for 5 d, the percentages of divided CD8$^+$ and CD4$^+$ T cells were obtained from loss of the CFSE signal in 7-aminoactinomycin D$^-$ cells (three independent experiments with CD8$^+$ T cells and with CD4$^+$ T cells involving different DC and T cell donors are shown). $*p < 0.05$ with unpaired *t* test. See Supplemental Fig. 3 for the FACS profiles. *B*, T cell/DC cocultures were collected for RNA extractions that were subjected to qRT-PCR for *IFNγ*, *Il13*, and *Il22* gene detection normalized to GAPDH. Levels of cytokine gene expression were calculated relative to the level of cytokine gene expression in the CD26$^+$ L-DC/T coculture of the respective DC donor (arbitrary units). The difficulty obtaining sufficient numbers of naive cells from the T cell and DC subset cells required that several naive T cell/L-DC couples, from independent sheep surgeries, were used to generate the qRT-PCR data. Each symbol shape represents a distinct L-DC/naive T cell donor. $**p < 0.01$; $***p < 0.001$, paired *t* test. *C*, CADM1 expression (thin line) on CD26$^+$CD1b$^+$ and CD26$^-$CD1b$^+$ gated DCs relative to control staining (thick line).

CD8α$^+$-like DC subsets in mouse, CD103 and CD207 (langerin) also show contrasting gene expression patterns between species, the first being expressed to higher levels on human pDCs, and the second on human BDCA1$^+$ DCs (data not shown). It is also well known that mouse pDCs express CD11c whereas human pDCs do not. In fact, CD11c relative expression across leukocyte subsets is strikingly different between mouse and human (data not shown). These examples illustrate how the use of one single molecule or even of a combination of a few markers can be very misleading when trying to establish the similarity between different cell types. This is not only the case for cross-species comparison but also for the classification of potentially novel cell types in a given species (22). Major differences can even be observed when comparing the same cell subset between different inbred mouse lines as illustrated by strain differences in CD207 and CD103 expression on splenic and lymph node CD8α$^+$ DCs (45, 52). In contrast, comparative genomics appears as the most potent and unbiased method to predict relationships between cell types, because it is based on the analysis of the whole gene expression program and hence allows evaluation of the overall proximity between cell types despite the specificities inherent to differences between their tissue of residency, between animal strains, or between vertebrate species. Comparative genomics also allows identification of the most relevant markers to identify a given cell type across species based on a highly selective and conserved expression profile, such as XCR1 for sheep CD26$^+$, mouse CD8α$^+$, and human BDCA3$^+$ DCs (24). Once predicted based on gene expression programs, the relationships between cell types can then be tested through functional analyses as performed here and through ontogenetic studies.

In addition to delineating similarities between DC subsets by using a global transcriptomic approach, we established that the sheep CD26$^+$ L-DCs were more efficient than their CD26$^-$ counterparts for activation of autologous CD8$^+$ T cells against soluble OVA. A comparative CD8$^+$ T cell activation with a MHC class I-specific OVA peptide could not be done, due to a lack of information on epitopic peptide in the sheep model and absence of data on the MHC class I typing in our breed. In any event, our data strongly support that this finding corresponds to a high efficacy for cross-presentation in the CD26$^+$ L-DCs because they selectively express characteristic features known to be associated with this function in mouse DCs, such as higher endosomal pH, efficient endosomal to cytosolic translocation of Ags, capture of apoptotic

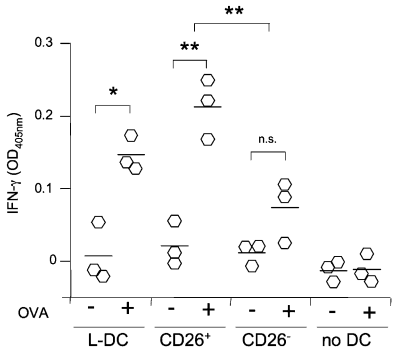


**FIGURE 6.** CD26$^+$ L-DCs are more efficient than CD26$^-$ L-DCs at stimulating specific autologous CD8$^+$ T cells in response to soluble OVA. Immunomagnetically selected L-DCs and CD26$^+$ and CD26$^-$ L-DCs (>85% purity, $5 \times 10^4$) were incubated with OVA (500 μg/ml). The next day, CFSE-labeled, OVA-immune efferent lymph-derived autologous enriched CD8$^+$ T cells ($5 \times 10^5$) were added to control and OVA-pulsed DCs. IFN-γ was measured in the supernatants, and OD at 405 nm is reported. $*p < 0.02$; $**p < 0.01$, unpaired *t* test. The results shown are from one representative experiment (sheep #62) out of two performed with different sheep.

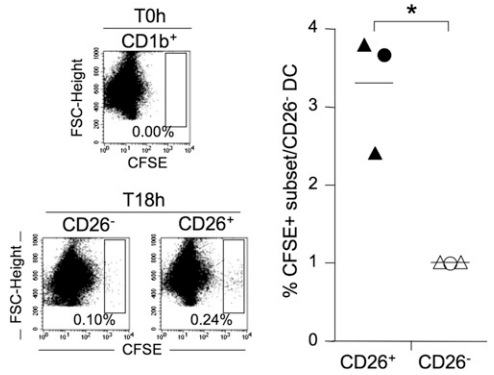


**FIGURE 8.** CD26$^+$ L-DCs dominantly capture apoptotic bodies in vivo. CFSE-labeled allogeneic apoptotic PBMCs ($3 \times 10^8$) were injected intradermally in the skin shoulder of afferently cannulated sheep; the post-injection overflow of the CFSE$^+$ PBMCs was eliminated at 3 h. The lymph cells were collected after 18 h and stained for CD1b and CD26 detection. The percentage of CSFE$^+$ cells within gated CD26$^+$CD1b$^+$ and CD26$^-$ CD1b$^+$ L-DCs was monitored before ($T = 0$) and after injection ($T = 18$ h). The ratio of the CFSE$^+$ capture in CD26$^+$ CD1b$^+$ versus CD26$^-$ CD1b$^+$ was calculated (sheep L-DCs: ●, #55; ▲, #70, used in two distinct experiments 1 wk apart). $*p < 0.05$, paired *t* test.

bodies, and specific high expression of CLEC9A. Due to the limitation of the sheep model, we had to evaluate the ability of CD26$^+$ DCs to activate CD8$^+$ T cells against exogenous Ags with autologous memory/effector T cells. Because cross-presentation by DCs is much less efficient with memory than naive CD8 T cells (53) and mature DCs are impaired in cross-priming (54), we can speculate that the intrinsic potential of the semimature CD26$^+$ L-DCs for CD8 T cell activation against exogenous Ag is even higher than that observed. Finally cross-priming could not be demonstrated after capture of exogenous apoptotic bodies, which is a too rare event among the collected L-DCs after injection (Fig. 8). Whereas the CD26$^-$ L-DCs were less efficient than the CD26$^+$ L-DCs for activation of allogeneic naive CD8$^+$ T cells and presentation of soluble OVA to CD8$^+$ T cells, they were similarly efficient at inducing *Il13* and *IFNγ* gene activation in allogeneic naive CD4$^+$ T cells (Fig. 5*B*). Of note, the lower efficacy of the CD26$^-$ L-DCs in CD8$^+$ T cell activation could not be attributed to culture-induced cell death in this subset because the ex vivo survival of CD26$^-$ L-DCs was slightly higher than that of CD26$^+$ L-DCs (95.8 versus 91.3% survival, respectively, after 24 h of culture). Furthermore, BTV-infected CD26$^-$ L-DCs performed as well as the CD26$^+$ L-DCs in BTV Ag presentation to specific CD8$^+$ T cells (Supplemental Fig. 4). Thus, CD26$^-$ L-DCs can be as good APCs as CD26$^+$ L-DCs in some situations but are clearly less efficient for allogeneic naive CD8$^+$ T cell stimulation and cross-presentation of OVA. It remains to be established to what respect they may perform better than the CD26$^+$ L-DCs.

Altogether, all of the genetic and functional features that distinguish sheep CD26$^+$ L-DCs from their CD26$^-$ counterparts establish a strong parallelism between the former and murine LT CD8α$^+$ or non-LT CD103$^+$ DCs. Hence, the CD26$^+$ L-DCs are functional homologues to mouse LT CD8α$^+$ and non-LT CD103$^+$

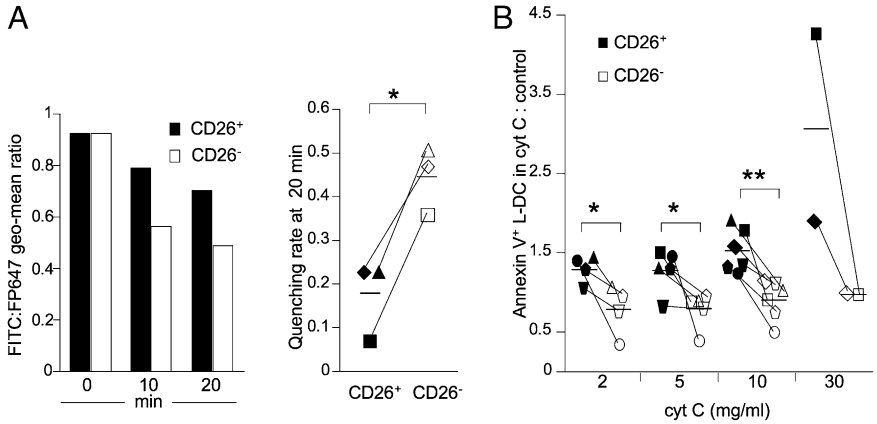


**FIGURE 7.** CD26$^+$ L-DCs show slower endosomal acidification and are more sensitive to cyt *c* treatment than CD26$^-$ L-DCs. *A*, LD lymph cells from sheep #33 were incubated with FITC-dextran 40,000 (FITC-dextran) and FluoProbes 647-dextran 40,000 (FP647-dextran) for 10 min at 37°C, extensively washed, and chased for 0–20 min at 37°C. Cells were placed on ice, stained with anti-CD26 and CD1b mAbs, and the geometric means of the FITC (pH-sensitive) and FluoProbes 647 (pH-insensitive) intensities were measured on the gated CD26$^+$CD1b$^+$ and CD26$^-$CD1b$^+$ L-DCs. The ratio of the mean fluorescence intensity emission between both dyes was determined at 0, 10, and 20 min (one measurement per time point in a representative experiment, *left panel*). In the *right panel*, the quenching rate at 20 min was calculated as 1 − [(FITC/FluoProbes 647 ratio at 20 min) / (FITC/FluoProbes 647 ratio at 0 min (pulse)] in three different sheep (sheep L-DCs: ■, #66; ▲, #70; ◆, #33; –, mean). $*p < 0.002$, paired *t* test. *B*, LD lymph cells were cultured alone (control) or with increasing doses of cyt *c* (2–30 mg/ml) overnight. They were then stained with anti-CD1b, anti-CD26, and annexin V and analyzed by FACS. The ratio of annexin V$^+$ cells in cyt *c*-treated versus control is reported for the CD26$^+$CD1b$^+$ and CD26$^+$CD1b$^-$ L-DCs from six experiments using three different sheep (●, #55; ■, #66; ◆, #33; –, mean). $*p < 0.05$; $**p < 0.01$.

Table III. *Similarities between sheep CD26$^+$/CD26$^-$ L-DCs, mouse CD8α$^+$/CD11b$^+$ spleen DCs, and human BDCA3$^+$/BDCA1$^+$ blood DCs*

| | Sheep CD26$^+$/CD26$^-$ L-DCs | Mouse CD8α$^+$/CD11b$^+$ Spleen DCs | Human BDCA3$^+$/BDCA1$^+$ Blood DCs |
|---|---|---|---|
| Global gene expression | GSEA sheep/mouse (25 and 15% of shared overexpressed orthologues)<br>GSEA sheep/human (26 and 35% of overexpressed orthologues)<br>GSEA mouse/human (18 and 36% of shared overexpressed orthologues) | | |
| CADM1 overexpression | RNA and protein | Protein and RNA (43) | Protein and RNA (43) |
| IL-22 induction | In MLR | Indirect evidence (43) | |
| Exogenous Ag presentation to CD8$^+$ T cells | To memory/effector CD8$^+$ T cells | To naive CD8$^+$ T cells (2, 9) | To memory/effector CD8$^+$ T cells (23–26) |
| Properties involved in cross-priming pathways | | | |
| Capture/maintenance of apoptotic bodies | In natural conditions and after injection (detection in lymph) | After injection (detection in spleen) (9) | Not known |
| CLEC9A overexpression | RNA | Protein and RNA (10) | Protein (10) |
| Controlled endosomal acidification | Yes | Yes (12) | Not known |
| Endosome to cytosol translocation of cyt *c* | Yes | Yes (13) | Not known |

DCs. Sheep could thus be a very suitable model for developing vaccine strategies targeting the cross-priming DC subsets, which could be evaluated by taking advantage of the possibility to challenge sheep with their natural intracellular pathogens such as lentiviruses and flaviviruses. Indeed chimeric Abs to CLEC9A or DEC205 could be built as single-chain variable fragment multibodies linked to microbial protein targets and used in vaccine strategies as in the mouse species (10, 55, 56). Of interest, the promise of chimeric Ab strategy in artiodactyls for the purpose of improved vaccination has been recently exemplified with an anti-sialoadhesin mAb in swine (57). Furthermore, XCR1, a cell surface chemokine receptor that is specifically expressed by CD8α-like DCs in the three species (mouse, human, and sheep) and endocytosed upon engagement, emerged as a promising molecular target candidate (this study and Ref. 24). The success of such novel vaccine strategies will depend on multiple parameters including the specificity of the target molecule expression on DCs and on the appropriate DC subset, the subcellular compartment of Ag delivery after endocytosis, and the maintenance of antigenicity after coupling with the Ab moiety.

A salient finding of our functional CD26$^+$/CD26$^-$ L-DC study is the specific induction by the CD26$^+$ L-DCs of the *Il22* gene expression in cocultures with naive CD4$^+$ and CD8$^+$ T cells. IL-22R is expressed exclusively by epithelial cells including skin, intestine, and lung (58). IL-22 has been implicated in epithelial cell homeostasis, infection, inflammation, and wound healing, with either a beneficial or negative effect on the epithelial integrity (46, 59–62). Recently, IL-22 has been found to be expressed by a distinct skin homing CCR4$^+$ CCR10$^+$ Th cell subset in human, which seems to be dedicated to skin patho-physiology (63, 64). IL-22 production was induced in naive CD4 T cells by human pDCs in an IL-23, IL-6, and TNF-α–dependant pathway. Yet, CD26$^+$ L-DCs strongly expressed IL-12p40, IL-6, and TNF-α as detected in the microarrays and confirmed by qRT-PCR (Fig. 3). Finally, as said above, APCs expressing CADM1 can engage CRTAM on CD8$^+$ T cells and hence promote IL-22 production by these lymphocytes in the mouse (43, 44). Thus, the combination of CAMD1, TNF-α, and IL-6 may be interplaying signals in IL-22 induction in CD4$^+$ and CD8$^+$ T cells by sheep CD26$^+$ L-DCs. This property found in sheep could interestingly apply to mouse CD8α$^+$ and human BDCA3$^+$ DCs, although this remains to be tested experimentally by taking into account parameters that may impact on IL-22 induction by CD8α-like DCs, such as the DC maturation status and the DC origin (migrated from skin or resident).

Overall, the sum of our data (Table III) establishes substantial similarities among sheep, human, and mouse DC subsets, suggesting that DC subset functional organization is conserved among phylogenetically distant mammals. It brings a definitive proof of concept that validates our comparative genomics approach to hunt for conserved functions based on conserved molecular pathways for DC subsets across several mammalian species. This work also leads us to consider renaming the different DC subsets, based on surface molecules expressed in common by the homologous DC subsets, such as CADM1$^+$ or XCR1$^+$ DCs for the CD8α$^+$ DC-like DCs and SIRP$^+$ DCs for the CD11b$^+$ DC-like DCs. It opens the way for the development of vaccine strategies targeting CD8α-like DCs in several mammalian species for the development of a new generation vaccines against zoonoses, infectious diseases of economical importance in livestock, and cancer in domestic carnivores, with the general goal to improve human and animal welfare. It remains to be determined whether DC subset organization, including pDC and conventional DC subsets, is found in other nonmammalian vertebrates and appeared at the same time as specific features of adaptive immunity.

## Acknowledgments

We thank Sanofi-Aventis for the generous gift of Lovenox. We thank Merial for providing inactivated BTV serotype 2 vaccine. We thank the Unité Commune d'Expérimentation Animale in Jouy-en-Josas, France, for providing sheep and caring for the cannulated sheep. We thank Florentina Pascale for help with the sheep. We thank Bertrand Schwartz, Bernard Malissen, and Bernard Charley for constructive input during writing of the manuscript. We thank the technicians of the Centre d'Imagerie Interventionnelle for help managing the surgery. We also thank the Iso Cell Express platform and Claudia Bevilacqua for support in qRT-PCR. We thank Bernard Jost and Doulaye Dembele from the Plate-forme Biopuces (Strasbourg, France) for performing the microarray experiment (www.microarrays.u-strasbg.fr).

## Disclosures

The authors have no financial conflicts of interest.

## References

1. Baranek, T., N. Zucchini, and M. Dalod. 2009. Plasmacytoid dendritic cells and the control of herpesvirus infections. *Viruses* 1: 383–419.
2. Segura, E., and J. A. Villadangos. 2009. Antigen presentation by dendritic cells in vivo. *Curr. Opin. Immunol.* 21: 105–110.
3. Crozat, K., R. Guiton, M. Guilliams, S. Henri, T. Baranek, I. Schwartz-Cornil, B. Malissen, and M. Dalod. 2010. Comparative genomics as a tool to reveal functional equivalences between human and mouse dendritic cell subsets. *Immunol. Rev.* 234: 177–198.
4. Young, L. J., N. S. Wilson, P. Schnorrer, A. Mount, R. J. Lundie, N. L. La Gruta, B. S. Crabb, G. T. Belz, W. R. Heath, and J. A. Villadangos. 2007. Dendritic cell preactivation impairs MHC class II presentation of vaccines and endogenous viral antigens. *Proc. Natl. Acad. Sci. USA* 104: 17753–17758.

5. Carter, R. W., C. Thompson, D. M. Reid, S. Y. Wong, and D. F. Tough. 2006. Preferential induction of CD4+ T cell responses through in vivo targeting of antigen to dendritic cell-associated C-type lectin-1. *J. Immunol.* 177: 2276–2284.
6. Dudziak, D., A. O. Kamphorst, G. F. Heidkamp, V. R. Buchholz, C. Trumpfheller, S. Yamazaki, C. Cheong, K. Liu, H. W. Lee, C. G. Park, et al. 2007. Differential antigen processing by dendritic cell subsets in vivo. *Science* 315: 107–111.
7. Heath, W. R., G. T. Belz, G. M. Behrens, C. M. Smith, S. P. Forehan, I. A. Parish, G. M. Davey, N. S. Wilson, F. R. Carbone, and J. A. Villadangos. 2004. Cross-presentation, dendritic cell subsets, and the generation of immunity to cellular antigens. *Immunol. Rev.* 199: 9–26.
8. Hochrein, H., K. Shortman, D. Vremec, B. Scott, P. Hertzog, and M. O'Keeffe. 2001. Differential production of IL-12, IFN-alpha, and IFN-gamma by mouse dendritic cell subsets. *J. Immunol.* 166: 5448–5455.
9. Iyoda, T., S. Shimoyama, K. Liu, Y. Omatsu, Y. Akiyama, Y. Maeda, K. Takahara, R. M. Steinman, and K. Inaba. 2002. The CD8+ dendritic cell subset selectively endocytoses dying cells in culture and in vivo. *J. Exp. Med.* 195: 1289–1302.
10. Caminschi, I., A. I. Proietto, F. Ahmet, S. Kitsoulis, J. Shin Teh, J. C. Lo, A. Rizzitelli, L. Wu, D. Vremec, S. L. van Dommelen, et al. 2008. The dendritic cell subtype-restricted C-type lectin Clec9A is a target for vaccine enhancement. *Blood* 112: 3264–3273.
11. Sancho, D., O. P. Joffre, A. M. Keller, N. C. Rogers, D. Martínez, P. Hernanz-Falcón, I. Rosewell, and C. Reis e Sousa. 2009. Identification of a dendritic cell receptor that couples sensing of necrosis to immunity. *Nature* 458: 899–903.
12. Savina, A., A. Peres, I. Cebrian, N. Carmo, C. Moita, N. Hacohen, L. F. Moita, and S. Amigorena. 2009. The small GTPase Rac2 controls phagosomal alkalinization and antigen crosspresentation selectively in CD8(+) dendritic cells. *Immunity* 30: 544–555.
13. Lin, M. L., Y. Zhan, A. I. Proietto, S. Prato, L. Wu, W. R. Heath, J. A. Villadangos, and A. M. Lew. 2008. Selective suicide of cross-presenting CD8+ dendritic cells by cytochrome c injection shows functional heterogeneity within this subset. *Proc. Natl. Acad. Sci. USA* 105: 3029–3034.
14. del Rio, M. L., J. I. Rodriguez-Barbosa, E. Kremmer, and R. Förster. 2007. CD103- and CD103+ bronchial lymph node dendritic cells are specialized in presenting and cross-presenting innocuous antigen to CD4+ and CD8+ T cells. *J. Immunol.* 178: 6861–6866.
15. Jaensson, E., H. Uronen-Hansson, O. Pabst, B. Eksteen, J. Tian, J. L. Coombes, P. L. Berg, T. Davidsson, F. Powrie, B. Johansson-Lindbom, and W. W. Agace. 2008. Small intestinal CD103+ dendritic cells display unique functional properties that are conserved between mice and humans. *J. Exp. Med.* 205: 2139–2149.
16. Ginhoux, F., M. P. Collin, M. Bogunovic, M. Abel, M. Leboeuf, J. Helft, J. Ochando, A. Kissenpfennig, B. Malissen, M. Grisotto, et al. 2007. Blood-derived dermal langerin+ dendritic cells survey the skin in the steady state. *J. Exp. Med.* 204: 3133–3146.
17. Bedoui, S., P. G. Whitney, J. Waithman, L. Eidsmo, L. Wakim, I. Caminschi, R. S. Allan, M. Wojtasiak, K. Shortman, F. R. Carbone, et al. 2009. Cross-presentation of viral and self antigens by skin-derived CD103(+) dendritic cells. *Nat. Immunol.* 10: 488–495.
18. Henri, S., L. F. Poulin, S. Tamoutounour, L. Ardouin, M. Guilliams, B. de Bovis, E. Devilard, C. Viret, H. Azukizawa, A. Kissenpfennig, and B. Malissen. 2010. CD207+ CD103+ dermal dendritic cells cross-present keratinocyte-derived antigens irrespective of the presence of Langerhans cells. *J. Exp. Med.* 207: 189–206.
19. Ginhoux, F., K. Liu, J. Helft, M. Bogunovic, M. Greter, D. Hashimoto, J. Price, N. Yin, J. Bromberg, S. A. Lira, et al. 2009. The origin and development of nonlymphoid tissue CD103+ DCs. *J. Exp. Med.* 206: 3115–3130.
20. Edelson, B. T., W. KC, R. Juang, M. Kohyama, L. A. Benoit, P. A. Klekotka, C. Moon, J. C. Albring, W. Ise, D. G. Michael, et al. 2010. Peripheral CD103+ dendritic cells form a unified subset developmentally related to CD8alpha+ conventional dendritic cells. *J. Exp. Med.* 207: 823–836.
21. Hildner, K., B. T. Edelson, W. E. Purtha, M. Diamond, H. Matsushita, M. Kohyama, B. Calderon, B. U. Schraml, E. R. Unanue, M. S. Diamond, et al. 2008. Batf3 deficiency reveals a critical role for CD8alpha+ dendritic cells in cytotoxic T cell immunity. *Science* 322: 1097–1100.
22. Robbins, S. H., T. Walzer, D. Dembélé, C. Thibault, A. Defays, G. Bessou, H. Xu, E. Vivier, M. Sellars, P. Pierre, et al. 2008. Novel insights into the relationships between dendritic cell subsets in human and mouse revealed by genome-wide expression profiling. *Genome Biol.* 9: R17.
23. Bachem, A., S. Güttler, E. Hartung, F. Ebstein, M. Schaefer, A. Tannert, A. Salama, K. Movassaghi, C. Opitz, H. W. Mages, et al. 2010. Superior antigen cross-presentation and XCR1 expression define human CD11c+CD141+ cells as homologues of mouse CD8+ dendritic cells. *J. Exp. Med.* 207: 1273–1281.
24. Crozat, K., R. Guiton, V. Contreras, V. Feuillet, C. A. Dutertre, E. Ventre, T. P. Vu Manh, T. Baranek, A. K. Storset, J. Marvel, et al. 2010. The XC chemokine receptor 1 is a conserved selective marker of mammalian cells homologous to mouse CD8alpha+ dendritic cells. *J. Exp. Med.* 207: 1283–1292.
25. Jongbloed, S. L., A. J. Kassianos, K. J. McDonald, G. J. Clark, X. Ju, C. E. Angel, C. J. Chen, P. R. Dunbar, R. B. Wadley, V. Jeet, et al. 2010. Human CD141+ (BDCA-3)+ dendritic cells (DCs) represent a unique myeloid DC subset that cross-presents necrotic cell antigens. *J. Exp. Med.* 207: 1247–1260.
26. Poulin, L. F., M. Salio, E. Griessinger, F. Anjos-Afonso, L. Craciun, J. L. Chen, A. M. Keller, O. Joffre, S. Zelenay, E. Nye, et al. 2010. Characterization of human DNGR-1+ BDCA3+ leukocytes as putative equivalents of mouse CD8alpha+ dendritic cells. *J. Exp. Med.* 207: 1261–1271.
27. Nishihara, H., M. Hasegawa, and N. Okada. 2006. Pegasoferae, an unexpected mammalian clade revealed by tracking ancient retroposon insertions. *Proc. Natl. Acad. Sci. USA* 103: 9929–9934.
28. Epardaud, M., M. Bonneau, F. Payot, C. Cordier, J. Mégret, C. Howard, and I. Schwartz-Cornil. 2004. Enrichment for a CD26hi SIRP- subset in lymph dendritic cells from the upper aero-digestive tract. *J. Leukoc. Biol.* 76: 553–561.
29. Bonneau, M., M. Epardaud, F. Payot, V. Niborski, M. I. Thoulouze, F. Bernex, B. Charley, S. Riffault, L. A. Guilloteau, and I. Schwartz-Cornil. 2006. Migratory monocytes and granulocytes are major lymphatic carriers of *Salmonella* from tissue to draining lymph node. *J. Leukoc. Biol.* 79: 268–276.
30. Howard, C. J., P. Sopp, J. Brownlie, L. S. Kwong, K. R. Parsons, and G. Taylor. 1997. Identification of two distinct populations of dendritic cells in afferent lymph that vary in their ability to stimulate T cells. *J. Immunol.* 159: 5372–5382.
31. Gohin, I. 1997. [The lymphatic system and its functioning in sheep]. *Vet. Res.* 28: 417–438.
32. Au, B., M. R. Boulton, P. P. Narini, C. A. McCulloch, and J. B. Hay. 1996. Lymph and interstitial fluid dynamics in labial gingival tissues of sheep. *J. Periodontal Res.* 31: 570–578.
33. Hemati, B., V. Contreras, C. Urien, M. Bonneau, H. H. Takamatsu, P. P. Mertens, E. Bréard, C. Sailleau, S. Zientara, and I. Schwartz-Cornil. 2009. Bluetongue virus targets conventional dendritic cells in skin lymph. *J. Virol.* 83: 8789–8799.
34. Pascale, F., V. Contreras, M. Bonneau, A. Courbet, S. Chilmonczyk, C. Bevilacqua, M. Epardaud, M. Epardaud, V. Niborski, et al. 2008. Plasmacytoid dendritic cells migrate in afferent skin lymph. *J. Immunol.* 180: 5963–5972.
35. Hope, J. C., L. S. Kwong, G. Entrican, S. Wattegedera, H. M. Vordermeier, P. Sopp, and C. J. Howard. 2002. Development of detection methods for ruminant interleukin (IL)-12. *J. Immunol. Methods* 266: 117–126.
36. Subramanian, A., H. Kuehn, J. Gould, P. Tamayo, and J. P. Mesirov. 2007. GSEA-P: a desktop application for Gene Set Enrichment Analysis. *Bioinformatics* 23: 3251–3253.
37. Lahoud, M. H., A. I. Proietto, K. H. Gartlan, S. Kitsoulis, J. Curtis, J. Wettenhall, M. Sofi, C. Daunt, M. O'keeffe, I. Caminschi, et al. 2006. Signal regulatory protein molecules are differentially expressed by CD8- dendritic cells. *J. Immunol.* 177: 372–382.
38. Dennis, G., Jr., B. T. Sherman, D. A. Hosack, J. Yang, W. Gao, H. C. Lane, and R. A. Lempicki. 2003. DAVID: Database for Annotation, Visualization, and Integrated Discovery. *Genome Biol.* 4: P3.
39. Mellor, A. L., B. Baban, P. Chandler, B. Marshall, K. Jhaver, A. Hansen, P. A. Koni, M. Iwashima, and D. H. Munn. 2003. Cutting edge: induced indoleamine 2,3 dioxygenase expression in dendritic cell subsets suppresses T cell clonal expansion. *J. Immunol.* 171: 1652–1655.
40. Vremec, D., and K. Shortman. 1997. Dendritic cell subtypes in mouse lymphoid organs: cross-correlation of surface markers, changes with incubation, and differences among thymus, spleen, and lymph nodes. *J. Immunol.* 159: 565–573.
41. Moser, M. 2001. Regulation of Th1/Th2 development by antigen-presenting cells in vivo. *Immunobiology* 204: 551–557.
42. Mackay, C. R., W. L. Marston, and L. Dudler. 1990. Naive and memory T cells show distinct pathways of lymphocyte recirculation. *J. Exp. Med.* 171: 801–817.
43. Galibert, L., G. S. Diemer, Z. Liu, R. S. Johnson, J. L. Smith, T. Walzer, M. R. Comeau, C. T. Rauch, M. F. Wolfson, R. A. Sorensen, et al. 2005. Nectin-like protein 2 defines a subset of T-cell zone dendritic cells and is a ligand for class-I-restricted T-cell-associated molecule. *J. Biol. Chem.* 280: 21955–21964.
44. Yeh, J. H., S. S. Sidhu, and A. C. Chan. 2008. Regulation of a late phase of T cell polarity and effector functions by Crtam. *Cell* 132: 846–859.
45. Qiu, C. H., Y. Miyake, H. Kaise, H. Kitamura, O. Ohara, and M. Tanaka. 2009. Novel subset of CD8{alpha}+ dendritic cells localized in the marginal zone is responsible for tolerance to cell-associated antigens. *J. Immunol.* 182: 4127–4136.
46. Eyerich, S., K. Eyerich, D. Pennino, T. Carbone, F. Nasorri, S. Pallotta, F. Cianfarani, T. Odorisio, C. Traidl-Hoffmann, H. Behrendt, et al. 2009. Th22 cells represent a distinct human T cell subset involved in epidermal immunity and remodeling. *J. Clin. Invest.* 119: 3573–3585.
47. Merad, M., and M. G. Manz. 2009. Dendritic cell homeostasis. *Blood* 113: 3418–3427.
48. Lindstedt, M., K. Lundberg, and C. A. Borrebaeck. 2005. Gene family clustering identifies functionally associated subsets of human in vivo blood and tonsillar dendritic cells. *J. Immunol.* 175: 4839–4846.
49. Belz, G. T., D. Vremec, M. Febbraio, L. Corcoran, K. Shortman, F. R. Carbone, and W. R. Heath. 2002. CD36 is differentially expressed by CD8+ splenic dendritic cells but is not required for cross-presentation in vivo. *J. Immunol.* 168: 6066–6070.
50. Schulz, O., D. J. Pennington, K. Hodivala-Dilke, M. Febbraio, and C. Reis e Sousa. 2002. CD36 or alphavbeta3 and alphavbeta5 integrins are not essential for MHC class I cross-presentation of cell-associated antigen by CD8 alpha+ murine dendritic cells. *J. Immunol.* 168: 6057–6065.
51. Albert, M. L., S. F. Pearce, L. M. Francisco, B. Sauter, P. Roy, R. L. Silverstein, and N. Bhardwaj. 1998. Immature dendritic cells phagocytose apoptotic cells via alphavbeta5 and CD36, and cross-present antigens to cytotoxic T lymphocytes. *J. Exp. Med.* 188: 1359–1368.
52. Shortman, K., and W. R. Heath. 2010. The CD8+ dendritic cell subset. *Immunol. Rev.* 234: 18–31.
53. Belz, G. T., S. Bedoui, F. Kupresanin, F. R. Carbone, and W. R. Heath. 2007. Minimal activation of memory CD8+ T cell by tissue-derived dendritic cells favors the stimulation of naive CD8+ T cells. *Nat. Immunol.* 8: 1060–1066.
54. Wilson, N. S., G. M. Behrens, R. J. Lundie, C. M. Smith, J. Waithman, L. Young, S. P. Forehan, A. Mount, R. J. Steptoe, K. D. Shortman, et al. 2006. Systemic activation of dendritic cells by Toll-like receptor ligands or malaria infection impairs cross-presentation and antiviral immunity. *Nat. Immunol.* 7: 165–172.
55. Nchinda, G., J. Kuroiwa, M. Oks, C. Trumpfheller, C. G. Park, Y. Huang, D. Hannaman, S. J. Schlesinger, O. Mizenina, M. C. Nussenzweig, et al. 2008.

The efficacy of DNA vaccination is enhanced in mice by targeting the encoded protein to dendritic cells. *J. Clin. Invest.* 118: 1427–1436.
56. Caminschi, I., M. H. Lahoud, and K. Shortman. 2009. Enhancing immune responses by targeting antigen to DC. *Eur. J. Immunol.* 39: 931–938.
57. Revilla, C., T. Poderoso, P. Martínez, B. Alvarez, L. López-Fuertes, F. Alonso, A. Ezquerra, and J. Domínguez. 2009. Targeting to porcine sialoadhesin receptor improves antigen presentation to T cells. *Vet. Res.* 40: 14.
58. Wolk, K., and R. Sabat. 2006. Interleukin-22: a novel T- and NK-cell derived cytokine that regulates the biology of tissue cells. *Cytokine Growth Factor Rev.* 17: 367–380.
59. Boniface, K., E. Guignouard, N. Pedretti, M. Garcia, A. Delwail, F. X. Bernard, F. Nau, G. Guillet, G. Dagregorio, H. Yssel, et al. 2007. A role for T cell-derived interleukin 22 in psoriatic skin inflammation. *Clin. Exp. Immunol.* 150: 407–415.
60. Brand, S., F. Beigel, T. Olszak, K. Zitzmann, S. T. Eichhorst, J. M. Otte, H. Diepolder, A. Marquardt, W. Jagla, A. Popp, et al. 2006. IL-22 is increased in active Crohn's disease and promotes proinflammatory gene expression and intestinal epithelial cell migration. *Am. J. Physiol. Gastrointest. Liver Physiol.* 290: G827–G838.
61. Zenewicz, L. A., G. D. Yancopoulos, D. M. Valenzuela, A. J. Murphy, M. Karow, and R. A. Flavell. 2007. Interleukin-22 but not interleukin-17 provides protection to hepatocytes during acute liver inflammation. *Immunity* 27: 647–659.
62. Sugimoto, K., A. Ogawa, E. Mizoguchi, Y. Shimomura, A. Andoh, A. K. Bhan, R. S. Blumberg, R. J. Xavier, and A. Mizoguchi. 2008. IL-22 ameliorates intestinal inflammation in a mouse model of ulcerative colitis. *J. Clin. Invest.* 118: 534–544.
63. Trifari, S., C. D. Kaplan, E. H. Tran, N. K. Crellin, and H. Spits. 2009. Identification of a human helper T cell population that has abundant production of interleukin 22 and is distinct from T(H)-17, T(H)1 and T(H)2 cells. *Nat. Immunol.* 10: 864–871.
64. Duhen, T., R. Geiger, D. Jarrossay, A. Lanzavecchia, and F. Sallusto. 2009. Production of interleukin 22 but not interleukin 17 by a subset of human skin-homing memory T cells. *Nat. Immunol.* 10: 857–863.